NIPER-415
Distribution Category UC-125

THERMODYNAMICS AND THE HYDRODENITROGENATION OF INDOLE

Part 1. Thermodynamic Properties of Indoline and 2-Methylindole

Part 2. Gibbs Energies of Reaction in the Hydrodenitrogenation of Indole

NIPER--415

Part 3. Thermodynamic Equilibria and Comparison with Literature Kinetic

DE89 000751

Topical Report

By
W. V. Steele
R. D. Chirico

June 1989

Work Performed Under Cooperative Agreement No. FC22-83FE60149

Prepared for
U. S. Department of Energy
Assistant Secretary for Fossil Energy

W. D. Peters, Project Manager
Bartlesville Project Office
P.O. Box 1398
Bartlesville, OK 74005

Prepared by
IIT Research Institute
National Institute for Petroleum and Energy Research
P. O. Box 2128
Bartlesville, OK 74005

EXECUTIVE SUMMARY

The average API gravity of the crude oil run to stills in the United States has dropped from approximately 34.2 in 1978 to 32.2 in 1987. That drop in gravity has been accompanied by an equivalent increase in the amount of petroleum coke exported by the U.S. When the cost of the oil imported and the price obtained for the coke are compared, it accounts for approximately **one billion dollars of the trade balance deficit per year.** The heavier crudes contain more carbon, sulfur, and nitrogen (heteroatom-containing compounds) than the benchmark West Texas intermediate. These heteroatom-containing compounds are difficult to remove. Processing of crudes containing increasing levels of nitrogen, oxygen and sulfur using present-day technology has produced fuels with high heteroatom contents and a tendency toward instability. The refractory nature of the heteroatom-containing compounds is the main reason for the increase in coke production. The full utilization of heavy oil to make quality transportation fuels requires an understanding of the chemistry and the thermodynamics of adding hydrogen to the feedstocks. The major goal of this research project is to aid in that understanding.

In earlier Topical Reports from NIPER it has been demonstrated that some of the hydrogenation reactions among heteroatomic species are reversible over a wide range of processing conditions. Consequently, a knowledge of the thermodynamic equilibria among species is essential for the proper interpretation of reaction data, for comparing different catalysts, and for accurate modelling of the overall reactions for such processes as hydrotreating or hydrocracking. Thermodynamics can be used to ascertain the relative stabilities of proposed intermediates, to determine if a given reaction is possible (and, if not, whether shifting the reaction conditions will make it so), and to determine specifically which reactions are reversible.

This topical report, discusses the role of thermodynamic equilibria in the HDN of indole. The report is divided into three parts. PART 1 gives details of experimental measurements made to determine the thermodynamic properties of indoline and 2-methylindole. PART 2 uses the experimental results in conjunction with group-additivity methodology to estimate the Gibbs energies of reaction for indole and possible intermediates in its HDN reaction. PART 3 uses Gibbs energies of reaction to investigate the HDN reaction. The discussion given in PART 3 covers each of three **key** questions concerning HDN reactions:

- What are the reaction networks? Alternatively, what are the stable intermediates formed?

- What are the reactivities of the various classes of nitrogen-containing compounds?
- Are the reaction networks and commonly accepted generalities about reactivities valid for broad groups of catalysts?

The investigations covered include; the role of the indole/indoline equilibrium, the interplay of thermodynamics and kinetics, and the effect of choice of catalyst on the aromaticity of the final products.

ABSTRACT

Ideal-gas thermodynamic properties for indoline and 2-methylindole based on accurate calorimetric measurements (between 300 to 500 K and 300 to 700 K, respectively) were determined; well into the range of typical chemical process temperatures. The calorimetrically derived values provide a firm basis for the prediction of thermodynamic properties for a large family of structures including many substituted indoles and indolines. Critical-temperature/density measurements obtained using a differential scanning calorimeter (DSC) are reported for 2-methylindole. A critical pressure and acentric factor are derived for 2-methylindole. Group-additivity estimation methods are employed to estimate the Gibbs energies of formation for the reactants, intermediates, and products in a reaction scheme for the hydrodenitrogenation (HDN) of indole. Thermodynamic equilibria calculations on the indole/indoline/hydrogen system are compared with experimental batch-reaction measurements reported in the literature. The interplay between thermodynamics and kinetics in the HDN of indole is discussed.

ACKNOWLEDGEMENTS

The authors gratefully acknowledge the financial support of the Office of Fossil Energy of the U.S. Department of Energy. This research has been funded within the Advanced Process Technology (APT) program as part of the Cooperative Agreement DE-FC22-83FE60149. The authors gratefully acknowledge Professor E. J. "Pete" Eisenbraun and his research group at Oklahoma State University for purification of the samples. The authors acknowledge the participation of I. A. Hossenlopp, A. Nguyen, and N. K. Smith in the measurements of the thermodynamic properties of indoline and 2-methylindole. M. Michael Strube is thanked for his assistance in the statistical-thermodynamics calculations on indole.

TABLE OF CONTENTS

TABLE OF CONTENTS (cont.)

TABLE OF CONTENTS (cont.)

LIST OF TABLES

LIST OF TABLES (cont.)

LIST OF FIGURES

INTRODUCTION §

Heterocyclic compounds in which the heteroatom N belongs to a 5- or 6-membered ring --- indoles, carbazoles, quinolines, and benzoquinolines --- constitute the major portion of the nitrogen compounds present in heavy oils and shale oils.[1,2]¶ The 5-membered ring systems are non-basic[3] due to the involvement of the nitrogen atom lone pair in the π-electron system of the pyrrole ring. In the 6-membered ring systems the nitrogen lone pair is not bound within the π-electron system of the pyridine ring, and hence, is available to bind with acids. These compounds are strong bases. Due to the different environments of the lone pair on the nitrogen atom in these systems, it is probable that each will react differently with a catalyst surface. Pyrrolic compounds are expected to bind to the catalyst surface through an extension of the π-electron system, whereas the pyridinic compounds are expected to bind through the nitrogen atom and its lone pair.

Catalytic hydrodenitrogenation (HDN) is a process in which organo-nitrogen compounds are removed from hydrocarbon feedstocks to produce processable, stable, and environmentally acceptable liquid fuels and lube base stocks. To date HDN has not been of great concern to refiners because of the small quantities of nitrogen present in conventional petroleum stocks. This situation, however, is changing as the need for the processing of heavier and lower-quality stocks (both rich in highly refractory nitrogen compounds) increases. For the present the catalyst technology used for hydrodesulfurization (HDS) has been adapted for HDN, despite the fact that it is not ideally suited for the purpose.[1]

Organic nitrogen and sulfur are commonly removed via reaction at 300 to 400° C and 50 to 150 atm. of hydrogen. Under these severe conditions, hydrogen is consumed not only in breaking carbon-nitrogen and carbon-sulfur bonds, but also in saturating aromatic components in the feed. Hydrogen consumption in excess of 1500 scf/bbl (standard cubic feet per barrel) is common in hydrotreating oil shale, while the amount required theoretically for selective heteroatom removal is only about 600 scf/bbl. Hence, the saving in expensive hydrogen used in processing could be enormous if a process for denitrogenation without saturation of the aromatic rings in the feedstock could be developed. Thus, interest in the development of more effective catalysts for

---

§ This research is funded by the Office of Fossil Energy of the U. S. Department of Energy within its Advanced Extraction and Process Technology (AEPT) research program.

¶ References are listed in numerical order at the end of this introduction.

HDN has grown, as witnessed by the rapid expansion of the patent literature in the area.[4]

Some key questions concerning hydrodenitrogenation reactions are:

- What are the reaction networks? Alternatively, what are the stable intermediates formed?
- What are the reactivities of the various classes of nitrogen-containing compounds?
- Are the reaction networks and commonly accepted generalities about reactivities valid for broad groups of catalysts?

Thermodynamics can be used to ascertain the relative stabilities of proposed reaction intermediates, to determine if a reaction is possible under given reaction conditions (and, if not, whether changing the reaction conditions will make it so), and to determine if the reactions are reversible.

The equilibrium thermodynamics associated with the hydrodenitrogenation of pyrrole has been discussed in previous reports in this research program.[5,6] This topical report, one of a series of reports[5-12] detailing the equilibrium thermodynamics associated with the hydrodenitrogenation (HDN) reactions of organic compounds present in fossil fuel materials, discusses the role of thermodynamic equilibria in the HDN of indole. The report is divided into three parts. PART 1 gives details of the experimental measurements made in these laboratories to determine the thermodynamic properties of indoline and 2-methylindole. PART 2 uses the results obtained in PART 1 in conjunction with group additivity methodology[13,14] to estimate the Gibbs energies of reaction for indole and the possible intermediates in its HDN reaction. PART 3 uses the results obtained in PART 2 to investigate the HDN reaction. The discussion given in PART 3 covers each of the three key questions concerning HDN reactions listed above. Topics include; the role of the indole/indoline equilibrium, the interplay of thermodynamic and kinetics, and the effect of choice of catalyst on the aromaticity of final products.

REFERENCES

1. Katzer, J. R.; Sivasubramanian, R. *Catal. Rev.-Sci. Eng.* **1979**, 20, 155.
2. Ledorix, M. J. *Catalysis (London)* **1985**, 7, 125.
3. Moore, R. T.; McCutchan, P.; Young, D. A. *Anal. Chem.* **1951**, 23, 1639.
4. Ho, T. C. *Catal. Rev.-Sci. Eng.* **1988**, 30, 117.
5. Steele, W. V.; Chirico, R. D.; Collier, W. B.; Hossenlopp, I. A.; Nguyen, A.; Strube, M. M. *Thermochemical and Thermophysical Properties of Organic*

Nitrogen Compounds Found in Fossil Materials. NIPER-188. Published by DOE Fossil Energy, Bartlesville Project Office. Available from NTIS Report No. DE-8687001204, November **1986.**

6. Steele, W. V.; Archer, D. G.; Chirico, R. D.; Strube, M. M. *Comparison of the Thermodynamics of Nitrogen and Sulfur Removal in Heavy Oil Upgrading. Part 1. Acyclic and Monocyclic Compounds* NIPER-264. July **1987.**
7. Steele, W. V.; Chirico, R. D.; Collier, W. B.; Harrison, R. H.; Gammon, B. E. *Assessment of Thermodynamic Data and Needs, Including Their Economic Impact, for Development of New Fossil Fuel Refining Processes.* NIPER-159. Published by DOE Fossil Energy, Bartlesville Project Office. Available from NTIS Report No. DE-86000298, June **1986.**
8. Messerly, J. F.; Todd, S. S.; Finke, H. L.; Good, W. D.; Gammon, B. E. *J. Chem. Thermodynamics* **1988**, 20, 209.
9. Steele, W. V.; Archer, D. G.; Chirico, R. D.; Collier, W. B.; Gammon, B. E.; Hossenlopp, I. A.; Nguyen, A.; Smith, N. K. *The Thermodynamic Properties of Quinoline and Isoquinoline.* NIPER-301. Published by DOE Fossil Energy, Bartlesville Project Office. Available from NTIS Report No. DE-88001218, November **1987.**
10. Steele, W. V.; Archer, D. G.; Chirico, R. D.; Collier, W. B.; Hossenlopp, I. A.; Nguyen, A.; Smith, N. K.; Gammon, B. E. *J. Chem. Thermodynamics* **1988**, 20, 1233.
11. Steele, W. V.; Chirico, R. D.; Hossenlopp, I. A.; Nguyen, A. *The Thermodynamic Properties of the Five Benzoquinolines.* NIPER-337. April **1988.** Published by DOE Fossil Energy, Bartlesville Project Office. Available from NTIS Report No. DE-88001240, October **1988.**
12. Steele, W. V.; Chirico, R. D.; Hossenlopp, I. A.; Nguyen, A.; Smith, N. K.; Gammon, B. E. *J. Chem. Thermodynamics* **1989**, 21, 81.
13. Benson, S. W. *Thermochemical Kinetics.* 2nd edition. Wiley: New York, **1976.**
14. Stull, D. R.; Westrum, E. F., Jr.; Sinke, G. C. *The Chemical Thermodynamics of Organic Compounds.* Wiley. New York. **1969.**

1.1. EXPERIMENTAL

MATERIALS

A commercial sample of indoline was purified in the following manner. The impure sample was treated with oxalic acid dihydrate in hot propan-2-ol (molecular proportions 1.4 to 1 to 50 for indoline, oxalic acid dihydrate, and propan-2-ol, respectively). The resulting oxalate was recrystallized from propan-2-ol, and cleaved using 2 $mol \cdot dm^{-3}$ KOH(aq). The liberated indoline was extracted with ether, dried (Na_2CO_3), filtered, and concentrated. Final purification was achieved by triple distillation at 320 K and 0.1 kPa through a Vigreaux column containing a tantalum spiral.

A commercial sample of 2-methylindole was purified in the same manner as that used for indoline. The final triple distillation was done at 327 K and 10 Pa. Glc analysis failed to detect any impurities in the calorimetric samples. The high purities (both 99.95 per cent) were confirmed in fractional-melting studies completed as part of the adiabatic heat-capacity studies.

The water used as a reference material in the ebulliometric vapor-pressure measurements was deionized and distilled from potassium permanganate. The decane used as a reference material for the ebulliometric measurements was purified by urea complexation, two recrystallizations of the complex, decomposition with water, extraction with ether, drying with $MgSO_4$, and distillation at 337 K and 1 kPa pressure.

PHYSICAL CONSTANTS AND STANDARDS

Molar values are reported in terms of $M = 119.1667\ g \cdot mol^{-1}$ for indoline and $M = 131.1777\ g \cdot mol^{-1}$ for 2-methylindole, respectively, based on the relative atomic masses of 1969[1]†§ and the gas constant, $R = 8.31441\ J \cdot K^{-1} \cdot mol^{-1}$, adopted by CODATA.[2] The platinum resistance thermometers used in these measurements were calibrated by comparison with standard thermometers whose constants were determined at the National Institute of Standards and Technology (NIST) formerly the National Bureau of Standards (NBS). All temperatures reported are in terms of the IPTS-68.[3] The platinum resistance thermometer used in the adiabatic heat-capacity studies was calibrated below 13.81 K using the method of McCrackin and Chang.[4] Measurements

† The 1969 relative atomic masses were used because the CODATA Recommended Key Values for Thermodynamics (reference 33) are based on them.

§ References are listed in numerical order at the end of this Part.

of mass, time, electrical resistance, and potential difference were made in terms of standards traceable to calibrations at NIST.

APPARATUS AND PROCEDURES

Combustion Calorimetry. The experimental procedures used in the combustion calorimetry of organic nitrogen compounds at the National Institute for Petroleum and Energy Research have been described.[5-7] A rotating-bomb calorimeter (laboratory designation BMR II)[8] and platinum-lined bombs (laboratory designations Pt-3b and Pt-5)[9] with internal volumes of 0.393_4 dm^3 and 0.393_0 dm^3, respectively, were used without rotation. Pt-3b was used in the 2-methylindole combustion measurements, and Pt-5 was used for the indoline combustions. The calorimetric samples of indoline were confined in borosilicate glass ampoules.[5,10] 2-Methylindole was found to quickly turn a deep brown on exposure to oxygen. Consequently, bags of polyester film[11] were used to confine the crystalline sample before combustion. For each experiment 1.0×10^{-3} dm^3 of water was added to the bomb, and the bomb was flushed and charged to 3.04 MPa with pure oxygen. Judicious choice of sample and auxiliary masses allowed the temperature rise in each combustion series and its corresponding calibration series to be the same in each experiment within 0.1 per cent. All experiments were completed very close to 298.15 K (within 0.01 K).

Temperatures were measured by quartz-crystal thermometry.[12,13] A computer was used to control the combustion experiments and record the results. The quartz-crystal thermometer was calibrated by comparison with a platinum resistance thermometer. Counts of the crystal oscillation were taken over periods of 100 s throughout the experiments. Integration of the time-temperature curve is inherent in the quartz-crystal thermometer readings.[14]

NBS benzoic acid (sample 39i) was used for calibration of the calorimeter; its specific energy of combustion is $-(26434.0 \pm 3.0)$ $J \cdot g^{-1}$ under certificate conditions. Conversion to standard states[15] gives $-(26413.7 \pm 3.0)$ $J \cdot g^{-1}$ for $\Delta_c U^\circ_m/M$, the specific energy of the idealized combustion reaction. Calibration experiments were interspersed with each series of measurements. Nitrogen oxides were not formed in the calibration experiments due to the high purity of the oxygen used and preliminary bomb flushing. The energy equivalent of the calorimeter ε(calor), obtained for each calibration series, was (16769.2 ± 0.6) $J \cdot K^{-1}$ (mean and standard deviation of the mean of six experiments) for 2-methylindole, and (16641.6 ± 0.7) $J \cdot K^{-1}$ (mean and standard deviation of the mean of six experiments) for the indoline measurements.

The auxiliary oil (laboratory designation TKL66) had the empirical formula $CH_{1.913}$. For this material $\Delta_c U^o_m/M$ was $-(46042.5\pm1.8)\ J\cdot g^{-1}$. For the cotton fuse, empirical formula $CH_{1.774}O_{0.887}$, $\Delta_c U^o_m/M$ was $-16945\ J\cdot g^{-1}$. The value for $\Delta_c U^o_m/M$ obtained for the polyester film, empirical formula $C_{10}H_8O_4$, was a function of the relative humidity (RH) in the laboratory during weighings:[11]

$$\{(\Delta_c U^o_m/M)/J\cdot g^{-1}\} = -22912.0 - 1.0560(RH)\ . \qquad (1.1)$$

Auxiliary information, necessary for reducing weights measured in air to masses, converting the energy of the actual bomb process to that of the isothermal process, and reducing to standard states,[15] included densities of $1067\ kg\cdot m^{-3}$ and $1070\ kg\cdot m^{-3}$, and estimated values of $1.7\ m^3\cdot K^{-1}$ and $0.5\ m^3\cdot K^{-1}$ for $(\delta V_m/\delta T)_p$ for indoline and 2-methylindole, respectively. The densities were obtained by weighing a pellet (2-methylindole) or ampoule (indoline) of known volume. Values of the molar heat capacities at 298.15 K for both compounds, used in the corrections to standard states, are given as part of the heat-capacity study results later in this report.

Nitric acid formed during the 2-methylindole and indoline combustions was determined by titration with standard sodium hydroxide.[16] Carbon dioxide was also recovered from the combustion products of each experiment. Anhydrous lithium hydroxide was used as absorbant.[6] The combustion products were checked for unburned carbon and other products of incomplete combustion, but none were detected. Carbon dioxide percentage recoveries were 100.002±0.005 (mean and standard deviation of the mean) for calibrations, 99.995±0.0.004 for the corresponding 2-methylindole combustions, 99.995±0.007 for calibrations, and 99.99±0.02 for the corresponding indoline combustions.

Ebulliometric Vapor-Pressure Measurements. The essential features of the ebulliometric equipment and procedures for vapor-pressure measurements are described in the literature.[17-19] The ebulliometers were used to reflux the substance under study with a standard of known vapor pressure under a common helium atmosphere. The boiling and condensation temperatures of the two substances were determined, and the vapor pressure was derived using the condensation temperature of the standard.[19]

The uncertainties in the temperature measurements for the ebulliometric vapor-pressure studies were 0.001 K. Uncertainties in the pressures were described adequately by the expression:

$$\sigma(p) = (0.001) \{ (dp_{ref}/dT)^2 + (dp_x/dT)^2 \}^{1/2} , \qquad (1.2)$$

where p_{ref} is the vapor pressure of the reference substance and p_x is the vapor pressure of the sample under study. Values of dp_{ref}/dT for the reference substances were calculated from fits of the Antoine equation[20] to vapor pressures of the reference materials (decane and water) reported in reference 19.

Inclined-piston Vapor-pressure Measurements. The equipment for vapor-pressure measurements with an inclined-piston gauge has been described by Douslin and McCullough,[21] and Douslin and Osborn.[22] Recent revisions to the equipment and procedures are given in references 23 and 24. Uncertainties in the pressures on the basis of estimated precision of measuring the mass, area, and angle of inclination of the piston, were adequately described by the expression:

$$\sigma(p) = 0.00015(p/Pa) + 0.200. \qquad (1.3)$$

The uncertainties in the temperatures were 0.001 K.

Adiabatic Heat-Capacity Calorimetry. Adiabatic heat-capacity and enthalpy measurements were made with a calorimetric system similar to that described by Huffman et al. [25-27] The four gold-plated copper adiabatic shields were controlled to within 1 mK by electronic controllers with proportional, derivative, and integral actions responding to imbalance signals from (copper+constantan) difference thermocouples. The calorimetric vessels and the loading and sealing procedures[25,23,24] have been described. The calorimeter characteristics and sealing conditions are given in table 1.1.¥

The temperature measurement system employed direct-current methods described previously.[25-27] In addition, some thermometer resistances were measured using self-balancing alternating-current resistance bridges (H. Tinsley & Co. Ltd.; Models 5840C and 5840D). Temperatures measured using both the d.c and a.c. systems agreed within 2 mK.

Energy measurement procedures were the same as those described for studies on quinoline.[23,24] Energies were measured to a precision of 0.01 per cent, and temperatures were measured to a precision of 0.0001 K. The energy increments to the filled calorimeters were corrected for enthalpy changes in the empty calorimeters, for

¥ Tables appear at the end of this Part.

the helium exchange gas, and for vaporization of the samples. The maximum correction to the measured energy for the helium exchange gas was approximately 0.16 per cent for indoline at 5.0 K, and 0.03 per cent for 2-methylindole at 11.3 K. The sizes of the other two corrections are indicated in table 1.1.

Differential Scanning Calorimetry (DSC) Measurements were made with a Perkin-Elmer DSC II which was fitted with a glove box to exclude air from the head. The calorimeter head was flushed with dry nitrogen. A Perkin-Elmer Intercooler II "Freon" refrigeration unit was used to remove energy from the calorimetric head.

The samples were confined in high-pressure cells fabricated at NIPER. The cells were made from 17-4 PH chromium nickel stainless steel (AISI#630). The features of the cells are described in Topical Reports NIPER-82 and NIPER-360.[28,29] The cells were sealed with gold gaskets in the form of washers. The internal volumes of the cells were determined from the masses of water held by the cells when immersed and sealed in distilled water. The heights of the cells were determined after sealing to correct the volumes for compression of the gold gaskets.

Oxygen is known to be a promoter of free radical formation leading to sample decomposition at high temperatures. Therefore, extreme care was used to exclude oxygen from both the samples and the cells. All cells were sealed in an atmosphere of dry nitrogen.

Measurements of the two-phase heat capacities (liquid plus vapor) were determined with a stepwise heating method described by Mraw and Naas.[30] Heating increments of 20 K at a heating rate of 5 K per minute were used. An integrating voltmeter was used to give an almost continuous integration of the imbalance signal from the DSC. A computer was programmed to step through the heat-equilibration-heat cycles, collect the imbalance signals from the voltmeter, and monitor the temperature from the DSC.

The temperature scale of the DSC was calibrated before each set of heat-capacity measurements by measurement of the melting temperatures of NIST Standard Reference Materials (SRM's) indium (429.78 K), tin (505.06 K), and lead (600.65 K). The energy scale of the DSC was assumed to be dependent upon temperature, scanning rate, and the gain settings for the instrument. Imbalance signals from the DSC were calibrated with sapphire using published heat-capacity values.[31] It was practical to work with the cells filled in the range of 0.5 to 1.5 times the critical density (approximately 20 to 50 per cent full at ambient temperature).

1.2. RESULTS

COMBUSTION CALORIMETRY

Typical combustion experiments for indoline and 2-methylindole are summarized in table 1.2. It is impractical to list summaries for each combustion, but values of $\Delta_c U^o_m/M$ for all the experiments are reported in table 1.3. All values of $\Delta_c U^o_m/M$ in table 1.3 refer to the reaction:

$$C_aH_bN\ (l \text{ or } c) + (a + b/4)\ O_2\ (g) = a\ CO_2\ (g) + b/2\ H_2O\ (l) + 1/2\ N_2\ (g). \quad (1.4)$$

Table 1.3 also gives derived values of the standard molar energy of combustion $\Delta_c U^o_m$, the standard molar enthalpy of combustion $\Delta_c H^o_m$, and the standard molar enthalpy of formation $\Delta_f H^o_m$, for indoline and 2-methylindole. Values of $\Delta_c U^o_m$ and $\Delta_c H^o_m$ refer to reaction **1.4**. The values of $\Delta_f H^o_m$ refer to reaction **1.5**:

$$aC(cr, \text{ graphite}) + b/2H_2\ (g) + 1/2N_2\ (g) = C_aH_bN\ (l \text{ or } c). \quad (1.5)$$

Uncertainties given in table 1.3 are the "uncertainty interval."[32] The enthalpies of formation of $CO_2(g)$ and $H_2O(l)$ were taken to be $-(393.51 \pm 0.13)$ and $-(285.830 \pm 0.042)$ kJ·mol^{-1}, respectively, as assigned by CODATA.[33]

VAPOR-PRESSURE MEASUREMENTS

Measured vapor pressures are listed in table 1.4. Following previous practice,[18] the ebulliometric measurement results were adjusted to common pressures. The common pressures, the condensation temperatures, and the difference between the boiling and condensation temperatures for the sample are reported in table 1.4.

Cox Equation Fit to Vapor Pressures. Previous studies[34] have shown that the Cox equation[35] can adequately represent measured vapor pressures from the triple-point pressure to 0.3 MPa, and can be used for extrapolation with good precision over a 50 K range. The Cox equation in the form:

$$\ln(p/p_{ref}) = \{1 - (T_{ref}/T)\}\exp\{A + B(T/K) + C(T/K)^2\}, \quad (1.6)$$

was fit to the experimental vapor pressures. p_{ref} was chosen to be 101.325 kPa so that T_{ref} was the normal-boiling temperature. The fitting procedure has been described.[23,24,19,36] Parameters derived from the fit for 2-methylindole and indoline are given in table 1.5. Details of the Cox equation fits are given in table 1.4.

Derived Enthalpies of Vaporization. Enthalpies of vaporization $\Delta_l^g H_m$ were derived from the Cox equation fits using the Clapeyron equation:

$$dp/dT = \Delta_l^g H_m / (T \Delta_l^g V_m) , \qquad (1.7)$$

where $\Delta_l^g V_m$ is the increase in molar volume from the liquid to the real vapor. In the calculation of $\Delta_l^g V_m$ estimates of the second virial coefficients were made using the correlation of Scott et al.[37] and liquid-phase densities of 1067 $kg \cdot m^{-3}$ at 298.15 K and 1020 $kg \cdot m^{-3}$ at 342 K for indoline and 2-methylindole, respectively. The liquid-phase densities were measured during the loading of the heat-capacity calorimeters. Generally, these density estimates have been found to be within 3 per cent of precisely determined values. Derived enthalpies of vaporization and entropies of compression are reported in table 1.6.

ADIABATIC HEAT-CAPACITY CALORIMETRY

Crystallization and Melting Studies. Crystallization of the 2-methylindole sample was initiated by slowly cooling the liquid sample (6 $K \cdot h^{-1}$) to approximately 3 K below its triple-point temperature. Complete crystallization was ensured by maintaining the sample under adiabatic conditions in the partially melted state (10 to 20 per cent liquid) until ordering of the crystals was complete, as evidenced by a cessation of spontaneous warming. The time required for warming to cease was approximately 20 h. Following the cessation of warming, the sample was cooled at an effective rate of 1 $K \cdot h^{-1}$ to crystallize the remaining liquid. Finally, the sample was thermally cycled between below 100 K and within 2 K of its triple-point temperature, where it was held for a minimum of 24 h to provide further tempering. All of the solid-phase measurements were performed upon crystals pre-treated in this manner.

Nucleation of the indoline crystals was initiated by either cooling slowly (4 $K \cdot h^{-1}$) to 35 K below the triple-point temperature or, by cooling rapidly (60 $K \cdot h^{-1}$) and initially forming the glass, followed by heating to roughly 10 K above the glass-transition temperature. Complete crystallization was ensured using the tempering methods described above for 2-methylindole.

The triple-point temperatures T_{tp} and sample purities were determined from measurements of equilibrium melting temperatures T(F) as a function of fraction F of the sample in the liquid state. Equilibrium melting temperatures were determined by measuring temperatures at approximately 300 s intervals for 0.75 to 1 h after an energy input and extrapolating to infinite time by assuming an exponential decay toward

the equilibrium value. The observed temperatures at 0.75 to 1 h after an energy input were invariably within 3 mK of the calculated equilibrium temperatures for F values listed in table 1.7.

The results for both indoline and 2-methylindole indicated the presence of solid-soluble impurities, and standard procedures[38] were used to derive the mole fractions of impurities, triple-point temperatures, and effective distribution coefficients for the impurities between the two phases. The results are summarized in table 1.7.

Phase Transformations and Enthalpy Measurements. Experimental molar enthalpy results are summarized in table 1.8. The table includes both phase-transition enthalpies and single-phase measurements, which serve as checks on the integration of the heat-capacity results. Corrections for pre-melting caused by impurities were made in these evaluations. Results with the same series number in tables 1.8 and 1.9 were taken without interruption of adiabatic conditions. Transformation of cr(I) to cr(II) in indoline occurred rapidly. The crystals were annealed at 46.2 K for 0.75 h prior to series 10 with no discernable increase in measured enthalpy.

Heat-Capacity Measurements. The experimental molar heat capacities under vapor-saturation pressure $C_{sat,m}$ are listed in table 1.9. The difference between $C_{p,m}$ and $C_{sat,m}$ is insignificant at 445 K, the highest measured temperature. Values in table 1.9 were corrected for effects of sample vaporization into the gas space of the calorimeter. The temperature increments were small enough to obviate the need for corrections for non-linear variation of $C_{sat,m}$ with temperature, except in the cr(II)-to-cr(I) transition region. The precision of the heat-capacity measurements ranged from approximately 2 per cent at 11 K to 0.2 per cent near 20 K and improved gradually to less than 0.1 per cent above 100 K, except in the solid phase near the triple-point temperature where equilibration times were long. The heat capacities in table 1.9 were not corrected for pre-melting, but the temperature increments are provided so that an independent calculation can be made.

Heat-capacity measurements in the liquid phase were routine with equilibrium being reached in less than 1 h. For the 2-methylindole sample, equilibration times for the crystal phase were less than 1 h for temperatures more than 50 K below the triple-point temperature. As the triple-point temperature was approached, the equilibration times increased gradually to a maximum of 6 h near 325 K. Analogous behavior was observed for the indoline sample with equilibration times increasing gradually from

1 h at 50 K below the triple-point temperature to 12 h near 245 K. No unusually long equilibration times were observed in the cr(II)-to-cr(I) transition region.

Figure 1.1 shows the experimental heat-capacity-against-temperature curve for indoline. The cr(II)-to-cr(I) region is expanded in figure 1.2. The horizontal bars represent the experimental temperature increments listed in table 1.9. For clarity, the single heat across the transition region of series 9 was not included in the figure. The uninterrupted curve is consistent with the individual average heat-capacity values shown in the figure, as well as with the overall transition enthalpy, as seen in table 1.8. The heat-capacity maximum was located at 47.5±0.2 K. The uncertainty in the temperature of the heat-capacity maximum does not significantly affect the derived entropy outside of the transition region. Heat-capacity values defining the uninterrupted curve are included in table 1.9.

Extrapolation to $T \rightarrow 0$ was made using a least-squares fit of the Debye heat-capacity equation to results below 18 K for 2-methylindole and below 12 K for indoline. The derived Debye characteristic temperatures were for 2-methylindole, $\Theta = 104.3$ K with 4.11 degrees of freedom; and for indoline, $\Theta = 82.9$ K with 2.89 degrees of freedom.

DIFFERENTIAL SCANNING CALORIMETRY

The theoretical background used in the derivation of $C_{p,m}$ values from the differential scanning calorimetric heat-capacity measurements was given in previous reports.[28,29] Attempts to determine heat capacities for indoline above 450 K were unsuccessful due to sample decomposition. In contrast, measurements were successfully completed on 2-methylindole over the complete liquid range from the triple-point temperature to the the critical point.

DSC Measurement Results. Table 1.10 lists the experimental two-phase heat capacities C_x^{II} for 2-methylindole obtained for four cell fillings. The temperature at which conversion to a single phase occurred was measured for six additional cell fillings. Table 1.11 reports the density (calculated from the mass of sample used and the cell volume) and the measured temperatures at which conversion to a single phase was observed for all ten fillings. A critical temperature of 810.0±2.0 K and a corresponding critical density of 300±3 $kg \cdot m^{-3}$ were derived for 2-methylindole using these results. Figure 1.3 shows the vapor-liquid coexistence region obtained from the DSC results. The curve given in figure 1.3 was drawn as an aid to the eye.

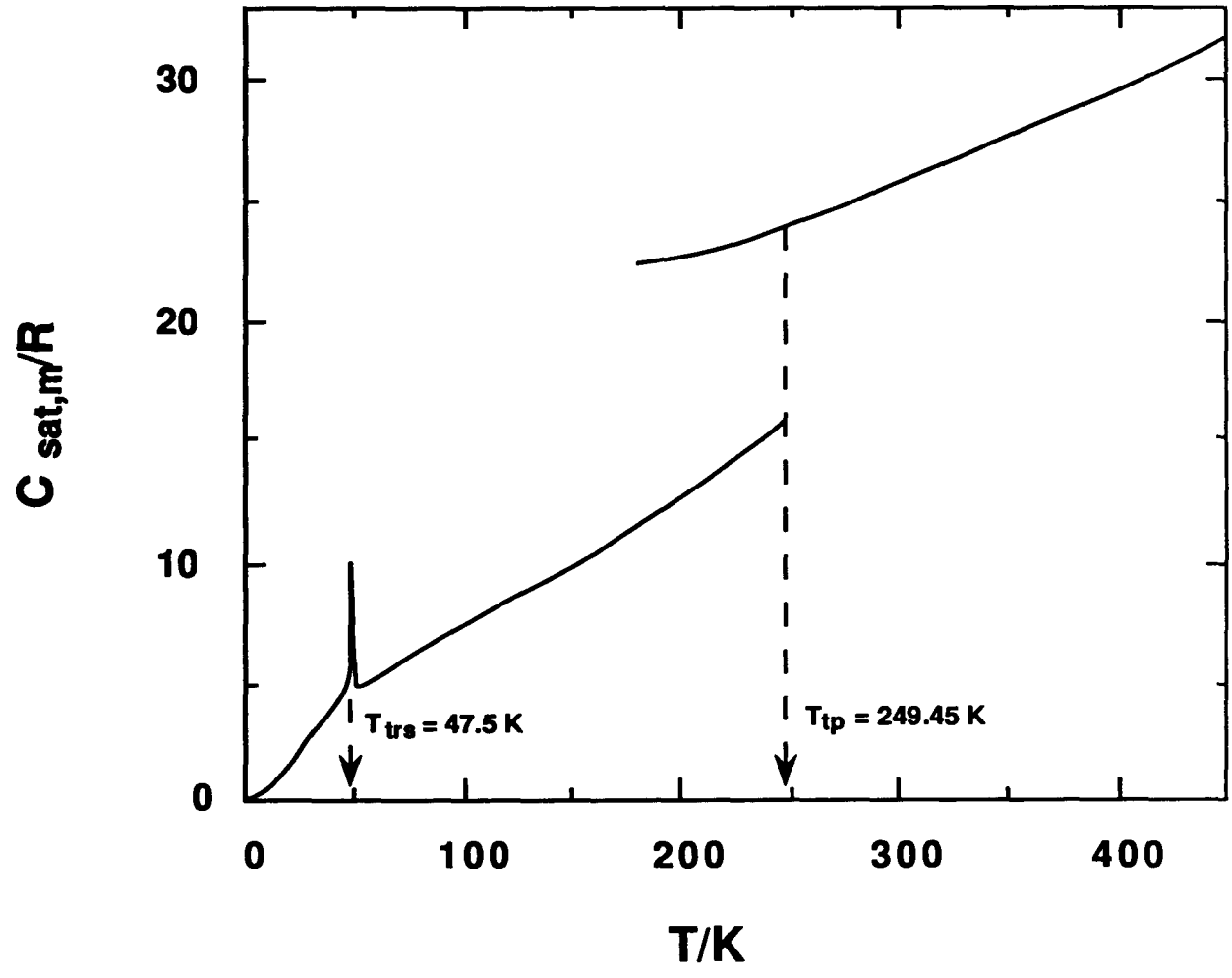

FIGURE 1.1 Heat capacity against temperature for indoline. The vertical lines indicate phase-transition temperatures.

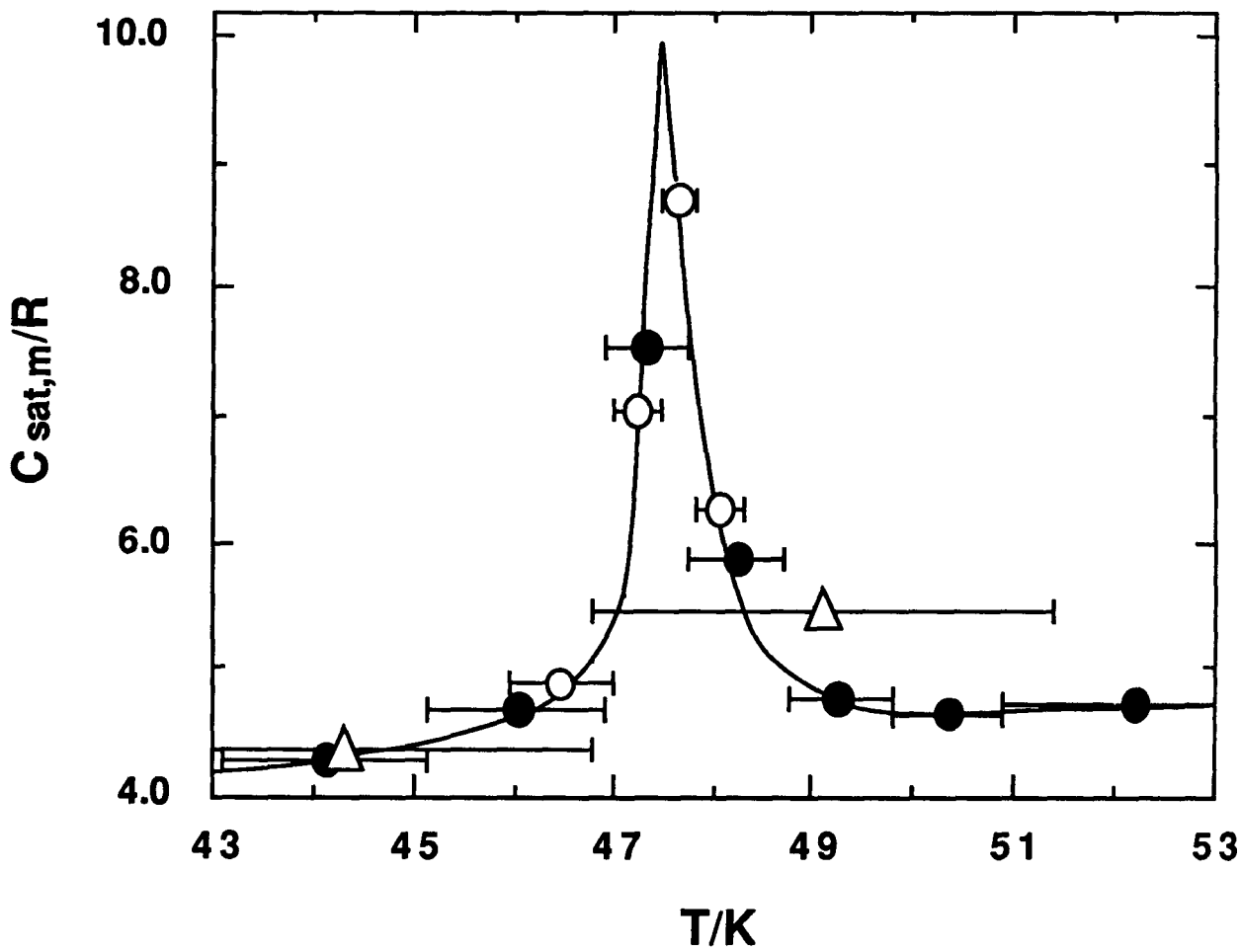

FIGURE 1.2 Experimental average heat capacities in the cr(II)-to-cr(I) transition region for indoline. △, Series 8; ●, series10; ○, series 11. The horizontal bars span the temperature increments associated with the average heat-capacity values. The uninterrupted curve is described in the text.

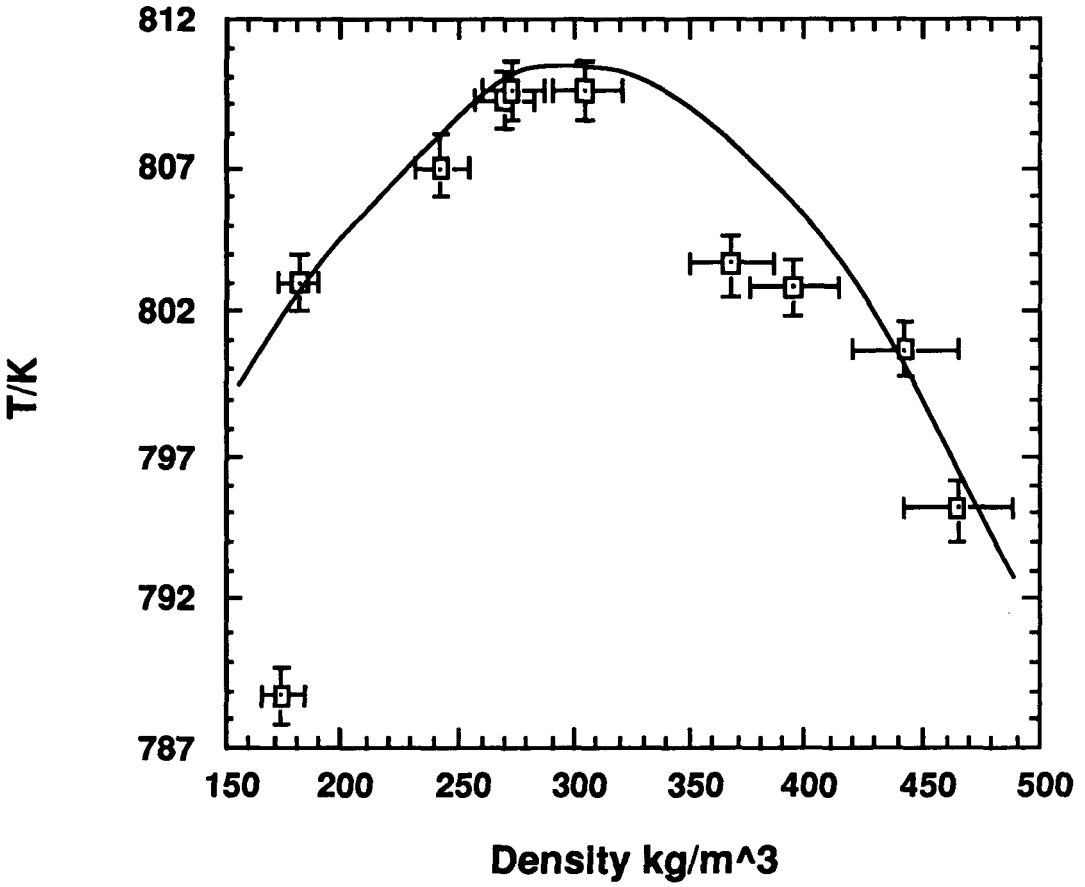

FIGURE 1.3 Vapor-liquid coexistence region for 2-methylindole.

Simultaneous Fit of Vapor-pressure and Two-phase Heat-capacity Results. The relationships given in reports NIPER-82 and NIPER-360[28,29] were used to derive values for the saturated heat capacity and estimate the critical pressure for 2-methylindole. The procedure required a simultaneous fit of the vapor pressures and two phase heat capacities for 2-methylindole.

The vapor-pressure measurements used in the fitting procedure described were those reported in table 1.4. The values of C_x^{II} were corrected to values at constant volume C_V^{II} with the thermal expansion of the cells expressed as:

$$V_x(T) \,/\, V_x(298\ K) = 1 + ay + by^2, \qquad (1.8)$$

where, y = (T – 298) K, a = 3.216 x 10^{-5} K^{-1}, b = 5.4 X 10^{-8} $K.^{-2}$ The values of C_V^{II} were used to derive functions for the derivatives $(d^2p/dT^2)_{sat}$, and $(d^2\mu/dT^2)_{sat}$ in non-linear least-squares simultaneous fits to the heat-capacity and vapor-pressure values. The Cox equation [35] was used to represent the vapor pressures in the form:

$$\ln(p/p_c) = (1 - 1/T_r)\ \exp\ (A + BT_r + CT_r^2)\,, \qquad (1.9)$$

with $T_r=T/T_c$, where T_c and p_c are the critical temperature and critical pressure. The functional form chosen for variation of the second derivative of the chemical potential with temperature was:

$$(d^2\mu/dT^2)_{sat} = \sum_{i=0}^{n} b_i\, x^i, \qquad (1.10)$$

where $x=(1 - T/T_c)$. In the fit the sum of the weighted squares in the following function was minimized:

$$\Delta = C_V^{II}/R - (VT/nR)(d^2p/dT^2)_{sat} + (T/R)(d^2\mu/dT^2)_{sat}\,. \qquad (1.11)$$

For the vapor-pressure fit, the functional forms of the weighting factors used are given in equations **(1.2)** and **(1.3)**. Within the heat-capacity data sets, the weighting factors were proportional to the square of the mass of sample used in the measurements. In addition, the weighting of the heat-capacity results relative to the vapor-pressures was an adjustable parameter in the fitting program. A weighting factor of 20 was used to increase the relative weights of the vapor-pressure measurements in the fit. This weighting factor reflected the higher precision of the vapor-pressure measurements in comparison to the experimental heat capacitiy measurements.

Table 1.12 lists the coefficients determined for 2-methylindole in the non-linear least-squares fit of the two-phase heat capacities from table 1.10 and the vapor pressures reported in table 1.4. The critical pressure was included as a variable in the non-linear least-squares analysis. Values of $C_{sat,m}$ were derived from $C_V^{II}(\rho=\rho_{sat})$ with the densities obtained using the corresponding-states equation in the form:[39,40]

$$(\rho/\rho_c) = 1.0 + 0.85\{1.0 - (T/T_c)\} + (1.692 + 0.986\omega)\{1.0 - (T/T_c)\}^{1/3}, \quad (12)$$

with $\rho_c = 300\ kg \cdot m^{-3}$, $T_c = 810.0$ K, and the acentric factor, $\omega = 0.454$. The acentric factor is defined as $\{-\log(p/p_c) - 1.0\}$, where p is the vapor pressure at $T_r = 0.7$ and p_c is the critical pressure. For 2-methylindole, values of 158 kPa and 4476 kPa were used for p and p_c, respectively. The Cox equation coefficients given in table 1.12 were used to calculate p. The results for $C_V^{II}(\rho = \rho_{sat})/R$ and $C_{sat,m}/R$ are reported in table 1.13.

THERMODYNAMIC PROPERTIES IN THE CONDENSED STATE

Condensed-phase entropies and enthalpies relative to those of the crystals at $T \rightarrow 0$ for the solid and liquid phases under vapor-saturation pressure are listed in table 1.14. These were derived by integration of the smoothed heat capacities corrected for pre-melting, together with the entropies and enthalpies of fusion. The heat capacities were smoothed with cubic-spline functions by least-squares fits to six points at a time and by requiring continuity in value, slope, and curvature at the junction of successive cubic functions. Due to limitations in the spline-function procedure, some acceptable values from tables 1.9 and 1.13 were not included in the fits, while in other regions graphical values were introduced to ensure that the second derivative of the heat capacity with respect to temperature was a smooth function of temperature. Pre-melting corrections were made using standard methods for a solid-insoluble impurity and the mole-fraction impurity values shown in table 1.1.

THERMODYNAMIC PROPERTIES IN THE IDEAL-GAS STATE

Enthalpies and entropies at selected temperatures for the ideal gas were calculated using values in tables 1.6 and 1.14, and are listed in columns 2 and 4 of table 1.15. The derived ideal-gas enthalpies and entropies were combined with the condensed-phase enthalpies of formation given in table 1.3 to calculate the enthalpies, entropies, and Gibbs energies of formation listed in columns 6, 7, and 8, respectively, of table 1.15. Enthalpies and entropies for equilibrium hydrogen and graphite were determined from

JANAF tables.[41] All uncertainties in table 1.15 represent one standard deviation, and include uncertainties in the properties of the elements as assessed in the JANAF tables.

1.3 SUMMARY

The thermodynamic properties reported here for 2-methylindole and indoline are the first reported for either compound. A search of the literature through February 1989 failed to find any experimental thermodynamic property determinations to compare with those obtained here. In the next section of this report (PART 2) the derived thermodynamic properties for 2-methylindole and indoline were used to estimate Gibbs energies in a reaction scheme for the hydrodenitrogenation (HDN) of indole.

1.4 REFERENCES

1. Commission on Atomic Weights. *Pure Appl. Chem.* **1970**, 21, 93.
2. *CODATA Bulletin No. 63,* November **1986**. International Council of Scientific Unions, Committee on Data for Science Technology.
3. Comitie International des Poids et Measures. *Metrologia* **1969**, 5, 35.
4. McCrackin, F. L.; Chang, S. S. *Rev. Sci. Instrum.* **1975**, 46, 550.
5. Good, W. D.; Moore, R. T. *J. Chem. Eng. Data* **1970**, 15, 150.
6. Good, W. D.; Smith, N. K. *J. Chem. Eng. Data* **1969**, 14, 102.
7. Good, W. D. *J. Chem. Eng. Data* **1969**, 14, 231.
8. Good, W. D.; Scott, D. W.; Waddington, G. *J. Phys. Chem.* **1956**, 60, 1080.
9. Good, W. D.; Douslin, D. R.; Scott, D. W.; George, A.; Lacina, J. L.; McCullough, J. P.; Waddington, G. *J. Phys. Chem.* **1959**, 63, 1133.
10. Guthrie, G. B.; Scott, D. W.; Hubbard, W. N.; Katz, C.; McCullough, J. P.; Gross, M. E.; Williamson, K. D.; Waddington, G. *J. Am. Chem. Soc.* **1952**, 74, 4662.
11. Good, W. D.; Scott, D. W.. *Experimental Thermochemistry* Vol II, editor Skinner, H. A. Interscience Publishers Inc., New York, **1962**, Chapt. 2, pp. 15-39.
12. Smith, N. K.; Stewart, R. C. Jr.; Osborn, A. G.; Scott, D. W. *J. Chem. Thermodynamics* **1980**, 12, 919.
13. Chirico, R. D.; Hossenlopp, I. A.; Nguyen, A.; Strube, M. M.; Steele, W. V. *Thermodynamic Studies Related to the Hydrogenation of Phenanthrene.* NIPER-247. Published by DOE Fossil Energy, Bartlesville Project Office. Available from NTIS Report No. DE-8687001252, April **1987**.
14. Goldberg, R. N.; Nuttall, R. N.; Prosen, E. J.; Brunetti, A. P. *NBS Report 10437,* U. S. Department of Commerce, National Bureau of Standards, June **1971**.
15. Hubbard, W. N.; Scott, D. W.; Waddington, G. *Experimental Thermochemistry* editor Rossini, F. D. Interscience Publishers Inc., New York, **1956**, Chapt. 5, pp. 75-128.
16. Smith, N. K.; Good, W. D. *J. Chem. Eng. Data* **1967**, 12, 572.
17. Swietoslawski, W. *Ebulliometric Measurements.* Reinhold Publishing Corp., New York, **1945**.
18. Osborn A. G.; Douslin, D. R. *J. Chem. Eng. Data* **1966**, 11, 502.
19. Chirico, R. D.; Nguyen, A.; Steele, W. V.; Strube, M. M.; Tsonopoulos, C. Accepted for publication *J. Chem. Eng. Data* , **1989**.

20. Antoine, C. C. R. *Acad. Sci.* **1888**, 107, 681.
21. Douslin, D. R.; McCullough, J. P. *BuMines RI* 6149, **1963**, pp. 11.
22. Douslin, D. R.; Osborn A. G. *J. Sci. Instrum.* **1965**, 42, 369.
23. Steele, W. V.; Archer, D. G.; Chirico, R. D.; Collier, W. B.; Gammon, B. E.; Hossenlopp, I. A.; Nguyen, A.; Smith, N. K. *The Thermodynamic Properties of Quinoline and Isoquinoline.* NIPER-301. Published by DOE Fossil Energy, Bartlesville Project Office. Available from NTIS Report No. DE-88001218, March **1988**.
24. Steele, W. V.; Archer, D. G.; Chirico, R. D.; Collier, W. B.; Hossenlopp, I. A.; Nguyen, A.; Smith, N. K.; Gammon, B. E. *J. Chem. Thermodynamics* **1988**, 20, 1233.
25. Huffman, H. M. *Chem Rev.* **1947**, 40, 1.
26. Ruehwein, R. A.; Huffman, H. M. *J. Am. Chem. Soc.* **1943**, 65, 1620.
27. Scott, D. W.; Douslin, D. R.; Gross, M. E.; Oliver, G. D.; Huffman, H. M. *J. Am. Chem. Soc.* **1952**, 74, 883.
28. Chirico, R. D.; Knipmeyer, S. E.; Nguyen, A.; Steele, W. V. "*Thermodynamic Properties of Biphenyl*" Topical Report NIPER-82, March **1989**.
29. Steele, W. V.; Chirico, R. D.; Knipmeyer, S. E.; Smith, N. K. High Temperature Heat-Capacity Measurements and Critical Property Determinations using a Differential Scanning Calorimeter. (Development of Methodology and Application to Pure Organic Compounds) Topical Report NIPER-360, October **1988**. Available from NTIS Report No. DE88001241.
30. Mraw, S. C.; Naas, D. F. *J. Chem. Thermodynamics* **1979**, 11, 567.
31. Ditmars, D. A.; Ishihara, S.; Chang, S. S.; Bemstein, G. *J. Res. Nat. Bur. Stds.* **1982**, 87, 159.
32. Rossini, F. D. *Experimental Thermochemistry*, editor Rossini, F. D. Interscience Publishers Inc., New York, **1956**, Chapt. 14, pp. 297-320.
33. CODATA Recommended Key Values for Thermodynamics 1977. See *J. Chem. Thermodynamics* **1978**, 10, 903.
34 Scott, D. W.; Osborn, A. G. *J. Phys. Chem.* **1979**, 83, 2714.
35. Cox, E. R. *Ind. Eng. Chem.* **1936**, 28, 613.
36. Gammon, B. E.; Callanan, J. E.; Hossenlopp, I. A.; Osborn, A. G.; Good, W. D. *Proceedings of the 8th Symposium on Thermophysical Properties* National Bureau of Standards, Gaithersburg, Md., June 15-19, **1981**.
37. Scott, D. W.; Finke, H. L.; Gross, M. E.; Guthrie, G. B.; Huffman, H. M. *J. Am. Chem. Soc.* **1950**, 72, 2424.

38. Mastrangelo, S. V. R.; Dornte, R. W. *J. Am. Chem. Soc.* **1955**, 77, 6200.
39. Pitzer, K. S.; Curl, R. F. Jr. *J. Am. Chem. Soc.* **1957**, 79, 2369.
40. Hales, J. L.; Townsend, R. *J. Chem. Thermodynamics* **1972**, 4, 763.
41. Chase, M. W., Jr.; Davies, C. A.; Cowney, J. R.; Frurip, D. J.; McDonald, R. A.; Syverud, A. N. *JANAF Thermochemical Tables Third edition. J. Phys. Chem. Ref. Data* **1985**, 14, supplement No. 1, 2 volumes.

TABLE 1.1. Calorimeter and sample characteristics; m is the sample mass, V_i is the internal volume of the calorimeter, T_{cal} is the temperature of the calorimeter when sealed, p_{cal} is the pressure of the helium and sample when sealed, r is the ratio of the heat capacity of the full calorimeter to that of the empty, T_{max} is the highest temperature of the measurements, $\delta C/C$ is the vaporization correction, and x_{pre} is the mole-fraction impurity used for pre-melting corrections.

	Indoline	**2-Methylindole**
	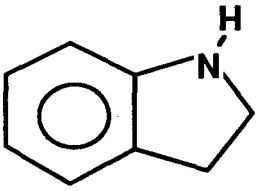	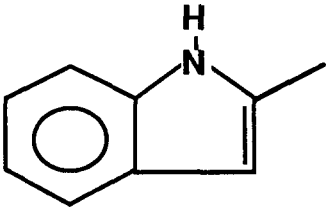
m/g	49.263	53.306
V_i(298.15 K)/cm^3	62.47	62.47
T_{cal}/K	294.6	299.0
p_{cal}/kPa	4.43	6.16
r(T_{max})	3.6	3.8
r_{min}	1.9	2.0
$10^2(\delta C/C)_{max}$	0.042	0.008
x_{pre}	0.0003	0.0002

TABLE 1.2. Typical combustion experiments at 298.15 K. [a] (p° = 101.325 kPa)

	Indoline	2-Methylindole
m'(compound)/g	0.932471	0.882620
m''(oil)/g	0.031700	0.0
m'''(polyester)/g	0.0	0.066859
m''''(fuse)/g	0.001267	0.002303
$n_i(H_2O)$/mol	0.05535	0.05535
m(Pt)/g	32.714	19.926
$\Delta T=(t_i - t_f + \Delta t_{corr})$/K	2.20044	2.04585
ε(calor)(ΔT)/J	−36618.8	−34307.3
ε(cont)(ΔT)/J [b]	−46.2	−38.4
ΔU_{ign}/J	0.7$_5$	0.7$_5$
$\Delta U_{dec}(HNO_3)$/J	28.3	56.9
ΔU(corr. to std. states)/J [c]	19.6	19.6
$-m''(\Delta_c U^\circ_m/M)$(oil)/J	1459.5	0.0
$-m'''(\Delta_c U^\circ_m/M)$(polyester)/J	0.0	1529.3
$-m''''(\Delta_c U^\circ_m/M)$(fuse)/J	21.5	39.0
$m'(\Delta_c U^\circ_m/M)$(compound)/J	−35135.4	−32700.1
$(\Delta_c U^\circ_m/M)$(compound)/J·g^{-1}	−37679.9	−37048.9

[a] The symbols and abbreviations of this table are those of reference 15 except as noted.

[b] $\varepsilon_i(cont)(t_i - 298.15\ K) + \varepsilon_f(cont)(298.15\ K - t_f + \Delta t_{corr})$

[c] Items 81 to 85, 87 to 90, 93, and 94 of the computational form of reference 15.

TABLE 1.3. Summary of experimental energies of combustion and molar thermochemical functions at T = 298.15 K and p° =101.325 kPa.

Indoline						
$\{(\Delta_c U^\circ_m/M)(\text{compound})\}/(J\cdot g^{-1})$						
−37679.9	−37668.1	−37679.5	−37669.9	−37684.8		
$\langle(\Delta_c U^\circ_m/M)/(J\cdot g^{-1})\rangle$					−37676.4±3.2	
$\Delta_c U^\circ_m/(kJ\cdot mol^{-1})$					−4489.78±1.00	
$\Delta_c H^\circ_m/(kJ\cdot mol^{-1})$					−4494.11±1.00	
$\Delta_f H^\circ_m/(kJ\cdot mol^{-1})$					59.80±1.08	
2-Methylindole						
$\{(\Delta_c U^\circ_m/M)(\text{compound})\}/(J\cdot g^{-1})$						
−37048.9	−37066.0	−37056.6	−37049.2	−37045.0	−37058.0	−37040.6
$\langle(\Delta_c U^\circ_m/M)/(J\cdot g^{-1})\rangle$					−37052.0±3.3	
$\Delta_c U^\circ_m/(kJ\cdot mol^{-1})$					−4860.40±1.08	
$\Delta_c H^\circ_m/(kJ\cdot mol^{-1})$					−4864.74±1.08	
$\Delta_f H^\circ_m/(kJ\cdot mol^{-1})$					36.91±1.16	

TABLE 1.4. Summary of vapor-pressure results; "IP" refers to measurements performed with the inclined-piston gauge, "water" or "decane" refers to which material was used as the standard in the reference ebulliometer, T is the temperature of the experimental inclined-piston pressure gauge measurements or, for ebulliometric measurements, of the condensation temperature of the sample, the pressure p for ebulliometric measurements was calculated from the condensation temperature of the reference substance, Δp is the difference of the calculated value of pressure from the observed value of pressure, σ_i is the propagated error calculated from equations (2) and (3), ΔT is the difference between the boiling and condensation temperatures ($T_{boil} - T_{cond}$) for the sample in the ebulliometer.

Method	$\frac{T}{K}$	$\frac{p}{kPa}$	$\frac{\Delta p}{kPa}$	$\frac{\sigma_i}{kPa}$	$\frac{\Delta T}{K}$
			Indoline		
decane	380.894	2.0000	−0.0005	0.0001	0.080
decane	387.309	2.6660	−0.0001	0.0002	0.070
decane	396.832	3.9999	0.0001	0.0002	0.062
decane	403.942	5.3330	0.0005	0.0003	0.056
decane	414.512	7.9989	0.0024	0.0004	0.052
decane	422.451	10.6661	0.0006	0.0006	0.041
decane	428.861	13.332	0.002	0.001	0.039
decane	435.527	16.665	0.000	0.001	0.035
water	441.045 [a]	19.933	0.010	0.001	0.037
decane	441.060	19.933	0.000	0.001	0.032
water	448.336 [a]	25.023	0.006	0.001	0.031
decane	448.350	25.023	−0.006	0.001	0.030
water	455.675	31.177	−0.002	0.002	0.028
water	463.058	38.565	−0.011	0.002	0.022
water	470.475	47.375	−0.007	0.002	0.021
water	477.940	57.817	−0.003	0.003	0.019
water	485.452	70.120	0.004	0.003	0.019
water	493.015	84.533	0.006	0.004	0.017
water	500.625	101.325	0.007	0.004	0.015
water	508.280	120.79	0.01	0.01	0.013
water	515.991	143.25	0.00	0.01	0.012

TABLE 1.4. Continued

Method	T / K	p / kPa	Δp / kPa	σ_i / kPa	ΔT / K
		Indoline (cont.)			
water	523.734	169.02	0.02	0.01	0.014
water	531.537	198.49	0.01	0.01	0.012
water	539.382	232.02	−0.01	0.01	0.012
water	547.269	270.02	−0.03	0.01	0.012
		2-Methylindole			
IP	340.001	0.0220	0.0001	0.0002	
IP	340.005 [a]	0.0220	0.0001	0.0002	
IP	350.003	0.0439	−0.0001	0.0002	
IP	360.000	0.0849	0.0002	0.0002	
IP	370.003	0.1564	0.0003	0.0002	
IP	370.003 [a]	0.1565	0.0004	0.0002	
IP	380.003	0.2769	0.0003	0.0002	
IP	390.004	0.4731	0.0003	0.0003	
IP	400.002	0.7822	0.0003	0.0003	
IP	410.007	1.2551	0.0000	0.0004	
IP	420.000	1.9581	−0.0004	0.0005	
IP	425.000	2.4229	−0.0004	0.0006	
IP	425.004 [a]	2.4230	−0.0006	0.0006	
IP	429.996	2.9790	−0.0003	0.0007	
decane	427.290	2.6660	0.0001	0.0002	0.070
decane	437.379	3.9999	0.0001	0.0002	0.039
decane	444.905	5.3330	−0.0007	0.0003	0.035
decane	456.076	7.9989	−0.0006	0.0004	0.017
decane	464.444	10.6661	−0.0003	0.0005	0.014
decane	471.202	13.332	0.000	0.001	0.010
decane	478.214	16.665	0.001	0.001	0.006
decane	484.034	19.933	0.002	0.001	0.005
decane	491.688	25.023	0.002	0.001	0.006
water	491.688 [a]	25.023	0.002	0.002	0.006
water	499.388	31.177	0.000	0.002	0.005

TABLE 1.4. Continued

Method	T / K	p / kPa	Δp / kPa	σ_i / kPa	ΔT / K
		2-Methylindole (cont.)			
water	507.125	38.565	0.000	0.002	0.004
water	514.904	47.375	−0.001	0.002	0.002
water	522.724	57.817	0.000	0.003	0.002
water	530.586	70.120	0.000	0.003	0.001
water	538.492	84.533	−0.001	0.004	0.002
water	546.439	101.325	0.002	0.004	0.003
water	554.431	120.79	0.00	0.005	0.003
water	562.465	143.25	0.00	0.01	0.003
water	570.538	169.02	0.00	0.01	0.004
water	578.656	198.49	0.00	0.01	0.005
water	586.812	232.02	0.01	0.01	0.009
water	595.011	270.02	0.00	0.01	0.009

[a] The value at this temperature was given zero weight in Cox equation fit.

TABLE 1.5. Cox equation coefficients

	Indoline	2-Methylindole
T_{ref}/K	500.628	546.439
P_{ref}/kPa	101.325	101.325
A	2.93300	3.01173
10^3B	−1.47504	−1.42712
10^6C	1.05763	0.91210
Range/K [a]	381 to 547	340 to 595

[a] Temperature range of the vapor pressures used in the fit.

TABLE 1.6. Enthalpies of vaporization and entropies of compression obtained from the Cox and Clapeyron equations [a]

T/K	$\Delta_l^g H_m/RK$	$\Delta S_{comp,m}/R$	T/K	$\Delta_l^g H_m/RK$	$\Delta S_{comp,m}/R$
		Indoline			
298.15 [b]	7332±19	−9.027±0.002	460.00	5982±18	−1.053±0.000
300.00 [b]	7315±18	−8.876±0.002	480.00	5822±26	−0.507±0.000
320.00 [b]	7138±10	−7.370±0.001	500.00	5660±36	−0.015±0.000
340.00 [b]	6963±5	−6.073±0.001	520.00	5495±48	0.433±0.000
360.00 [b]	6793±3	−4.948±0.000	540.00	5326±64	0.841±0.000
380.00	6626±3	−3.966±0.000	560.00 [b]	5150±83	1.215±0.000
400.00	6463±5	−3.102±0.000	580.00 [b]	4967±105	1.560±0.000
420.00	6301±8	−2.339±0.000	600.00 [b]	4774±131	1.879±0.000
440.00	6142±12	−1.660±0.000			
		2-Methylindole			
290.00 [b,c]	8896±18	−12.828±0.001	500.00	6878±19	−1.162±0.000
298.15 [b,c]	8812±15	−11.993±0.001	520.00	6695±28	−0.630±0.000
300.00 [b,c]	8793±14	−11.811±0.001	540.00	6510±39	−0.146±0.000
320.00 [b,c]	8586±9	−10.000±0.001	560.00	6320±52	0.295±0.000
340.00	8383±6	−8.440±0.000	580.00	6124±68	0.698±0.000
360.00	8183±3	−7.086±0.000	600.00 [b]	5921±88	1.070±0.000
380.00	7988±2	−5.904±0.000	620.00 [b]	5708±111	1.413±0.000
400.00	7796±2	−4.865±0.000	640.00 [b]	5483±139	1.732±0.000
420.00	7608±3	−3.946±0.000	660.00 [b]	5243±171	2.028±0.000
440.00	7423±5	−3.130±0.000	680.00 [b]	4985±208	2.306±0.000
460.00	7241±8	−2.402±0.000	700.00 [b]	4704±250	2.567±0.000
480.00	7059±13	−1.750±0.000			

[a] $\Delta S_{comp}/R = \ln(p/p^\circ)$ where p° = 101.325 kPa and R = 8.31441 $J \cdot K^{-1} \cdot mol^{-1}$.

[b] Values at this temperature were calculated with extrapolated vapor pressures determined from the fitted Cox coefficients.

[c] Values for supercooled liquid.

TABLE 1.7 Melting-study summaries; F is the fraction melted at observed temperature T(F), T_{tp} is the triple-point temperature, x is the mole-fraction impurity, and K_d is the distribution coefficient for the impurity as defined in reference 38

	F	T(F)/K	F	T(F)/K
	Indoline		**2-Methylindole**	
	0.201	249.357	0.140	331.849
	0.350	249.394	0.278	331.906
	0.498	249.409	0.463	331.933
	0.647	249.418	0.601	331.944
	0.796	249.425	0.740	331.951
T_{tp}/K	249.45		331.982	
x	0.00053		0.00046	
K_d	0.050		0.045	

TABLE 1.8 Experimental enthalpy measurements (R = 8.31441 $J \cdot K^{-1} \cdot mol^{-1}$)

N [a]	h [b]	T_i / K	T_f / K	T_{trs} / K	$\Delta_{tot}H_m$ [c] / R·K	$\Delta_{trs}H_m$ [d] / R·K
			Indoline			
			cr(II) to cr(I)			
8	2	41.813	51.409	47.5	46.93	−0.01
9	1	38.962	51.987		60.64	−0.03
10	4	45.158	49.813		25.44	0.00
11	4	45.956	48.308		14.48	0.02
					Average:	0.00
			Single-phase measurements in cr(I)			
4	1	211.724	244.856		477.66	0.01
5	1	120.976	190.117		698.99	−0.02
5	1	190.123	234.743		597.17	−0.16
12	1	52.560	109.045		357.62	0.07
13	1	84.520	179.575		847.93	−0.04
14	1	202.742	242.771		562.15	−0.40
			cr(I) to liquid			
3	6	243.440	252.072	249.45	1326.43	1169.40
4	2	244.773	254.205		1357.12	1169.30
14	2	242.869	252.753		1351.76	1169.53
					Average:	1169.41
			Single-phase measurements in liquid			
15	4	193.073	251.279		1351.33	−0.88
16	1	260.194	290.485		752.70	0.09
18	1	319.570	392.080		2018.13	0.08
18	1	392.045	441.999		1508.77	−0.38

TABLE 1.8 Continued

N [a]	h [b]	T_i / K	T_f / K	T_{trs} / K	$\Delta_{tot}H_m$ [c] / R·K	$\Delta_{trs}H_m$ [d] / R·K
			2–Methylindole			
			Single–phase measurements in cr			
6	1	54.855	151.984		813.09	0.33
6	1	152.125	245.447		1340.28	–0.03
6	1	245.395	305.740		1177.61	0.40
6	1	305.674	325.585		446.61	–0.04
			cr to liquid			
3	4	325.422	337.544	331.982	2100.58	1785.52
4	7	324.503	333.581		2006.12	1784.74
6	2	325.583	334.830		2017.29	1784.78
					Average:	1785.02
			Single–phase measurements in liquid			
8	1	344.273	417.226		2289.51	–0.21
8	1	417.184	437.321		677.97	–0.09

[a] Adiabatic series number

[b] Number of heating increments

[c] $\Delta_{tot}H_m$ is the molar energy input from the initial temperature T_i to the final temperature T_f.

[d] $\Delta_{trs}H_m$ is the net molar enthalpy of transition at the transition temperature T_{trs}.

TABLE 1.9. Experimental molar heat capacities at vapor-saturation pressure ($R = 8.31441\ J \cdot K^{-1} \cdot mol^{-1}$)

N[a]	<T>/K	ΔT/K	$C_{sat,m}/R$[b]	N[a]	<T>/K	ΔT/K	$C_{sat,m}/R$[b]
			Indoline				
			cr(II)				
11	5.025	0.8441	0.046	8	21.749	2.2725	1.778
11	5.912	0.8686	0.079	8	24.183	2.5906	2.079
11	6.844	1.0294	0.125	8	26.852	2.7403	2.395
11	7.896	1.0850	0.190	8	29.734	3.0221	2.719
11	8.976	1.0674	0.273	8	32.856	3.2283	3.065
11	10.029	1.0377	0.368	8	36.208	3.4796	3.429
11	11.111	1.1190	0.475	9	37.021	3.8818	3.514
8	11.809	1.0981	0.548	10	39.467	3.1969	3.765
11	12.293	1.2452	0.602	8	39.880	3.8625	3.808
8	13.007	1.2826	0.683	10	42.077	2.0201	4.039
11	13.596	1.3571	0.752	10	44.123	2.0690	4.273
8	14.370	1.4593	0.847	8	44.305	4.9841	4.351
11	15.026	1.5032	0.931	9	45.475	13.0247	4.656
8	15.920	1.6323	1.044	10	46.039	1.7608	4.689
11	16.606	1.6709	1.127	11	46.492	1.0719	4.876
8	17.650	1.8323	1.259	11	47.246	0.4368	7.057
11	18.374	1.8536	1.352	10	47.339	0.8373	7.524
8	19.589	2.0462	1.505	11	47.653	0.3771	8.715
11	20.329	2.0465	1.599	8	49.103	4.6116	5.474
			cr(I)				
11	48.074	0.4668	6.271	2	136.536	9.3324	9.109
10	48.244	0.9711	5.868	2	146.022	9.6052	9.587
10	49.272	1.0816	4.774	2	155.676	9.6728	10.086
10	50.353	1.0781	4.665	2	165.361	9.6717	10.602
10	52.203	2.6188	4.726	2	175.047	9.6794	11.130
8	54.478	6.1349	4.851	14	182.422	9.7816	11.541
5	55.074	4.6093	4.885	2	184.751	9.7121	11.683

TABLE 1.9. Continued

N[a]	<T>/K	ΔT/K	$C_{sat,m}$[b]/R	N[a]	<T>/K	ΔT/K	$C_{sat,m}$[b]/R
			cr(I) (continued)				
5	60.168	5.4982	5.200	6	188.328	15.5488	11.892
5	65.998	6.1004	5.550	14	195.081	15.2367	12.294
5	72.589	6.9640	5.930	6	203.945	15.5839	12.844
5	79.871	7.5562	6.322	2	204.191	9.7135	12.863
5	87.961	8.4356	6.741	3	204.883	9.8629	12.907
2	89.178	8.6351	6.817	2	213.913	9.7252	13.481
5	96.915	9.1808	7.186	3	214.894	10.0582	13.543
2	98.229	9.3640	7.252	6	219.615	15.6059	13.855
5	106.354	9.6681	7.644	3	226.186	12.5205	14.334
2	107.668	9.3958	7.710	6	235.067	15.2206	15.008
5	116.080	9.7574	8.111	3	237.964	11.0524	15.249
2	117.159	9.5096	8.163	5	240.594	11.8643	15.665
2	126.727	9.5719	8.628				
			liquid				
15	187.167	3.8976	22.458	17	296.553	9.5528	25.600
15	191.125	3.8893	22.528	16	304.567	9.4854	25.890
16	230.880	4.9618	23.424	17	307.279	11.3543	25.989
16	237.525	8.3206	23.623	17	319.523	13.1015	26.445
16	246.282	9.2028	23.887	17	332.562	12.9512	26.934
16	255.540	9.3193	24.183	17	345.900	13.7136	27.444
3	256.159	8.1829	24.207	17	359.983	14.4501	27.987
14	257.311	9.1111	24.244	17	374.338	14.2728	28.546
4	258.460	8.5344	24.280	17	388.536	14.1031	29.098
1	264.894	8.1220	24.483	17	402.549	13.9411	29.644
1	273.819	9.7542	24.791	17	416.382	13.7857	30.181
1	283.969	9.6649	25.143	17	429.211	11.9373	30.689
16	295.154	9.3730	25.545	17	440.042	9.8376	31.118

TABLE 1.9. Continued

N[a]	<T>/K	ΔT/K	$C_{sat,m}$[b]/R	N[a]	<T>/K	ΔT/K	$C_{sat,m}$[b]/R
			2-Methylindole				
			cr				
5	11.266	1.1282	0.387	1	134.699	10.0375	10.331
5	12.408	1.1287	0.501	1	144.760	10.0797	10.946
5	13.643	1.3351	0.634	1	154.889	10.1407	11.558
5	15.089	1.5437	0.808	1	165.038	10.1153	12.213
5	16.688	1.6473	1.005	1	175.177	10.1588	12.833
5	18.467	1.8999	1.232	1	185.352	10.1867	13.477
5	20.500	2.1570	1.490	1	195.544	10.1985	14.130
5	22.780	2.3910	1.783	1	205.750	10.2166	14.789
5	25.309	2.6602	2.100	1	215.952	10.1930	15.455
5	27.775	2.2638	2.396	1	226.129	10.1744	16.130
5	30.595	3.3852	2.721	1	236.271	10.1649	16.804
5	34.103	3.6459	3.118	1	246.373	10.1836	17.481
5	37.861	3.8706	3.518	1	256.589	10.2729	18.180
5	41.971	4.3504	3.924	1	266.917	10.4100	18.886
5	46.603	4.9076	4.359	2	276.466	10.6292	19.552
5	51.656	5.1970	4.804	1	277.408	10.6089	19.614
1	53.693	5.2102	4.986	2	287.094	10.5874	20.339
5	57.119	5.7305	5.253	1	288.083	10.7909	20.398
1	59.065	5.4873	5.413	2	297.667	10.5632	21.094
1	64.846	6.0405	5.855	1	298.882	10.8616	21.196
1	71.309	6.8537	6.330	3	302.779	8.9868	21.483
1	78.481	7.4706	6.829	4	304.070	7.9645	21.567
1	86.418	8.3124	7.351	2	308.060	10.3215	21.877
1	95.271	9.2383	7.917	1	309.638	10.7124	22.009
1	104.877	9.7505	8.510	3	311.798	8.9973	22.194
1	114.719	9.9083	9.117	4	312.153	8.0263	22.224
1	124.677	9.9956	9.723	4	320.348	8.2253	22.981

TABLE 1.9. Continued

N[a]	<T>/K	ΔT/K	$C_{sat,m}$[b]/R	N[a]	<T>/K	ΔT/K	$C_{sat,m}$[b]/R
			liquid				
4	337.648	8.1520	29.123	7	374.882	12.7363	31.104
6	338.899	8.1489	29.194	7	387.531	12.5661	31.758
3	341.591	8.1125	29.343	7	399.915	12.4125	32.366
3	349.913	8.5492	29.780	7	412.636	13.0802	32.991
7	350.335	10.4764	29.807	7	425.613	12.9266	33.597
7	362.049	12.9192	30.437	7	437.021	9.9791	34.121

[a] Adiabatic series number.

[b] Average heat capacity for a temperature increment of ΔT with a mean temperature <T>.

TABLE 1.10. Experimental C_x^{II}/R values for 2-methylindole

(R = 8.31441 $J \cdot K^{-1} \cdot mol^{-1}$)

mass / g	0.009526	0.020098	0.014971	0.012690
Vol. of cell / cm^3 [a]	0.0547	0.0547	0.0547	0.0547
T/K	C_x^{II}/R	C_x^{II}/R	C_x^{II}/R	C_x^{II}/R
355.0	30.03	30.01	29.98	30.09
375.0	31.20	31.15	30.96	30.84
395.0	32.17	32.10	32.00	32.00
415.0	33.14	33.18	33.11	33.12
435.0	34.45		34.01	34.21
455.0	35.36	34.98	34.46	35.25
475.0	36.38	35.82	35.91	36.24
495.0	37.77	36.89	37.19	36.96
515.0	38.92		38.12	38.00
535.0	40.01	38.56	39.17	39.24
555.0	41.18	39.88	40.22	40.38
575.0	42.63	40.55	40.98	41.68
595.0	43.64	41.84	42.33	42.52
615.0	45.52	42.40	43.06	43.63
635.0	47.12	43.14	44.47	45.20
655.0	48.62	44.33	45.83	46.51
675.0	50.49	44.84	47.24	47.51
695.0	52.04	45.71	48.02	48.78
715.0	54.98	46.77	48.82	50.76
735.0		47.83	50.57	51.99
755.0	59.89	49.31	51.44	54.39

[a] Volume measured at 298.15 K.

TABLE 1.11. Temperatures for the conversion from two phases to a single phase for 2-methylindole

ρ/kg·m^{-3}	T/K
176.5	788.8
183.3	803.0
238.4	807.0
264.7	809.2
268.7	809.6
299.5	809.6
360.9	803.6
399.3	802.9
433.9	800.7
470.4	795.1

TABLE 1.12. Parameters for equations (1.9) and (1.10) for 2-methylindole

	A	2.63930	b_1	−0.42774	
	B	−1.48266	b_2	−0.48575	
	C	0.92713	b_3	0.0	
T_c	810.0 K	P_c	4476 kPa	ρ_c	300 kg·m^{-3}

TABLE 1.13. Values of $C_V^{II}(\rho = \rho_{sat})/R$ and $C_{sat,m}/R$ for 2-methylindole

T/K	$C_V^{II}(\rho = \rho_{sat}/R$	$C_{sat,m}/R$	T/K	$C_V^{II}(\rho = \rho_{sat})/R$	$C_{sat,m}/R$
400.0	64.4	64.4	600.0	81.1	81.3
420.0	66.5	66.5	620.0	82.5	82.7
440.0	68.4	68.4	640.0	83.8	84.1
460.0	70.3	70.3	660.0	85.1	85.6
480.0	72.0	72.0	680.0	86.4	87.1
500.0	73.7	73.7	700.0	87.8	88.9
520.0	75.3	75.3	720.0	89.4	91.0
540.0	76.8	76.9	740.0	91.2	93.6
560.0	78.3	78.4	760.0	93.4	97.5
580.0	79.7	79.8			

TABLE 1.14. Molar thermodynamic functions at vapor-saturation pressure ($R = 8.31441\ J \cdot K^{-1} \cdot mol^{-1}$)

$\frac{T}{K}$	$\frac{C_{sat,m}}{R}$	$\frac{\Delta_0^T S_m^o}{R}$	$\frac{\Delta_0^T H_m^o}{RT}$	$\frac{T}{K}$	$\frac{C_{sat,m}}{R}$	$\frac{\Delta_0^T S_m^o}{R}$	$\frac{\Delta_0^T H_m^o}{RT}$
			Indoline				
			cr(II)				
5.000 [a]	0.049	0.016	0.012	35.000	3.299	2.058	1.347
6.000	0.085	0.028	0.021	40.000	3.820	2.532	1.624
7.000	0.133	0.045	0.034	42.000	4.028	2.724	1.733
8.000	0.198	0.067	0.050	44.000	4.256	2.916	1.842
9.000	0.275	0.094	0.071	45.000	4.409	3.014	1.898
10.000	0.365	0.128	0.095	46.000	4.656	3.113	1.955
12.000	0.570	0.212	0.157	47.000	5.328	3.218	2.017
14.000	0.802	0.317	0.232	47.100	5.536	3.230	2.025
16.000	1.052	0.440	0.319	47.200	5.989	3.242	2.032
18.000	1.304	0.579	0.414	47.300	7.273	3.256	2.042
20.000	1.558	0.729	0.516	47.400	8.587	3.273	2.054
25.000	2.177	1.144	0.787	47.500	9.900	3.292	2.070
30.000	2.749	1.592	1.067				
			cr(I)				
47.500	9.900	3.292	2.070	100.000	7.337	7.649	4.136
47.600	9.188	3.313	2.086	110.000	7.819	8.371	4.449
47.700	8.476	3.331	2.100	120.000	8.300	9.072	4.750
47.800	7.764	3.348	2.113	130.000	8.788	9.755	5.042
47.900	7.041	3.364	2.124	140.000	9.282	10.424	5.327
48.000	6.361	3.378	2.133	150.000	9.791	11.082	5.608
48.500	5.195	3.436	2.170	160.000	10.315	11.731	5.885
49.000	4.839	3.488	2.198	170.000	10.853	12.372	6.162
49.500	4.700	3.536	2.224	180.000	11.411	13.008	6.438
50.000	4.660	3.583	2.249	190.000	11.985	13.640	6.715
51.000	4.677	3.675	2.296	200.000	12.592	14.270	6.993

TABLE 1.14. Continued

$\frac{T}{K}$	$\frac{C_{sat,m}}{R}$	$\frac{\Delta_0^T S_m^o}{R}$	$\frac{\Delta_0^T H_m^o}{RT}$	$\frac{T}{K}$	$\frac{C_{sat,m}}{R}$	$\frac{\Delta_0^T S_m^o}{R}$	$\frac{\Delta_0^T H_m^o}{RT}$
			cr(I) (continued)				
52.000	4.715	3.766	2.342	210.000	13.217	14.900	7.275
56.000	4.941	4.124	2.519	220.000	13.858	15.529	7.559
60.000	5.188	4.473	2.689	230.000	14.525	16.160	7.847
70.000	5.783	5.318	3.089	240.000	15.204	16.793	8.140
80.000	6.330	6.127	3.461	249.450 [a]	15.852	17.392	8.420
90.000	6.844	6.902	3.808				
			liquid				
185.000 [a]	22.424	15.182	9.621	340.000	27.218	29.968	16.422
190.000	22.506	15.781	9.959	350.000	27.602	30.762	16.736
200.000 [b]	22.693	16.940	10.591	360.000	27.988	31.545	17.043
210.000 [b]	22.901	18.052	11.172	370.000	28.377	32.317	17.344
220.000 [b]	23.135	19.123	11.710	380.000	28.766	33.079	17.640
230.000	23.401	20.157	12.213	390.000	29.155	33.832	17.930
240.000	23.696	21.159	12.685	400.000	29.545	34.575	18.216
249.450	23.989	22.080	13.108	410.000	29.933	35.309	18.497
250.000	24.006	22.133	13.132	420.000	30.324	36.035	18.774
260.000	24.327	23.081	13.556	430.000	30.720	36.753	19.047
270.000	24.658	24.005	13.961	440.000	31.117	37.464	19.317
280.000	25.004	24.908	14.349	450.000 [a]	31.513	38.168	19.583
290.000	25.360	25.792	14.723	460.000 [a]	31.908	38.865	19.847
298.150	25.657	26.499	15.018	470.000 [a]	32.304	39.555	20.108
300.000	25.724	26.657	15.083	480.000 [a]	32.700	40.239	20.366
310.000	26.089	27.507	15.432	490.000 [a]	33.096	40.918	20.622
320.000	26.462	28.341	15.771	500.000 [a]	33.492	41.590	20.875
330.000	26.837	29.161	16.101				

TABLE 1.14. Continued

$\frac{T}{K}$	$\frac{C_{sat,m}}{R}$	$\frac{\Delta_0^T S_m^o}{R}$	$\frac{\Delta_0^T H_m^o}{RT}$	$\frac{T}{K}$	$\frac{C_{sat,m}}{R}$	$\frac{\Delta_0^T S_m^o}{R}$	$\frac{\Delta_0^T H_m^o}{RT}$
			2-Methylindole				
10.000 [a]	0.277	0.094	0.070	150.000	11.261	11.577	6.116
12.000	0.459	0.160	0.119	160.000	11.887	12.324	6.457
14.000	0.676	0.246	0.183	170.000	12.517	13.063	6.795
16.000	0.919	0.352	0.260	180.000	13.137	13.796	7.130
18.000	1.172	0.475	0.347	190.000	13.774	14.524	7.463
20.000	1.427	0.612	0.442	200.000	14.416	15.246	7.795
25.000	2.062	0.999	0.703	210.000	15.064	15.965	8.126
30.000	2.654	1.428	0.979	220.000	15.721	16.681	8.456
35.000	3.216	1.880	1.259	230.000	16.384	17.395	8.786
40.000	3.732	2.343	1.537	240.000	17.050	18.106	9.117
45.000	4.211	2.811	1.807	250.000	17.725	18.816	9.447
50.000	4.659	3.278	2.070	260.000	18.408	19.524	9.779
60.000	5.486	4.202	2.572	270.000	19.093	20.232	10.111
70.000	6.235	5.105	3.043	280.000	19.804	20.939	10.444
80.000	6.931	5.983	3.486	290.000	20.533	21.647	10.780
90.000	7.582	6.838	3.905	298.150	21.109	22.224	11.054
100.000	8.210	7.669	4.304	300.000	21.241	22.355	11.117
110.000	8.827	8.481	4.687	310.000	21.996	23.063	11.455
120.000	9.439	9.275	5.058	320.000	22.769	23.774	11.797
130.000	10.046	10.054	5.418	330.000 [a]	23.560	24.486	12.141
140.000	10.655	10.821	5.771	331.982 [a]	23.720	24.628	12.210
			liquid				
298.150 [a]	27.004	27.007	16.415	500.000	37.020	43.430	22.786
300.000 [a]	27.104	27.174	16.481	510.000	37.472	44.168	23.070
310.000 [a]	27.640	28.071	16.832	520.000	37.902	44.899	23.351
320.000 [a]	28.179	28.957	17.178	530.000	38.304	45.625	23.629
330.000 [a]	28.713	29.833	17.520	540.000	38.690	46.345	23.905

TABLE 1.14. Continued

$\frac{T}{K}$	$\frac{C_{sat,m}}{R}$	$\frac{\Delta_0^T S_m^o}{R}$	$\frac{\Delta_0^T H_m^o}{RT}$	$\frac{T}{K}$	$\frac{C_{sat,m}}{R}$	$\frac{\Delta_0^T S_m^o}{R}$	$\frac{\Delta_0^T H_m^o}{RT}$
			liquid (continued)				
331.982 [a]	28.819	30.005	17.587	550.000	39.069	47.058	24.177
340.000	29.255	30.698	17.857	560.000	39.443	47.765	24.446
350.000	29.786	31.554	18.190	570.000	39.812	48.467	24.712
360.000	30.325	32.400	18.520	580.000	40.177	49.162	24.976
370.000	30.852	33.238	18.846	590.000	40.536	49.852	25.237
380.000	31.371	34.068	19.169	600.000	40.893	50.537	25.495
390.000	31.880	34.890	19.488	610.000	41.249	51.215	25.750
400.000	32.372	35.703	19.804	620.000	41.605	51.889	26.003
410.000	32.862	36.508	20.117	630.000	41.960	52.558	26.253
420.000	33.337	37.306	20.426	640.000	42.317	53.221	26.501
430.000	33.799	38.096	20.731	650.000	42.682	53.880	26.748
440.000	34.258	38.878	21.034	660.000	43.055	54.535	26.992
450.000	34.717	39.653	21.333	670.000	43.438	55.185	27.234
460.000	35.177	40.421	21.629	680.000	43.841	55.831	27.476
470.000	35.636	41.183	21.922	690.000	44.269	56.474	27.716
480.000	36.095	41.938	22.212	700.000	44.721	57.115	27.956
490.000	36.557	42.687	22.500				

[a] Values at this temperature were calculated with graphically extrapolated heat capacities.

[b] Interpolated values.

TABLE 1.15. Thermodynamic properties in the ideal-gas state
($R = 8.31441\ J \cdot K^{-1} \cdot mol^{-1}$ and $p^\circ = 101.325\ kPa$)

$\frac{T}{K}$		$\frac{\Delta_0^T H_m^\circ}{R\,T}$	$\frac{\Delta_{imp} H_m^\circ}{R\,T}$ [a]	$\frac{\Delta_0^T S_m^\circ}{R}$	$\frac{\Delta_{imp} S_m^\circ}{R}$ [b]	$\frac{\Delta_f H_m^\circ}{R\,T}$	$\frac{\Delta_f S_m^\circ}{R}$	$\frac{\Delta_f G_m^\circ}{R\,T}$
				2-Methylindole				
290.00	c,d	46.800±0.064	0.000	44.111±0.066	0.000	51.48±0.25	−43.55±0.23	95.04±0.32
298.15	c,d	45.967±0.053	0.000	44.566±0.057	0.000	49.80±0.24	−43.83±0.23	93.63±0.33
300.00	c,d	45.787±0.049	0.000	44.669±0.055	0.000	49.43±0.24	−43.89±0.23	93.33±0.33
320.00	c,d	44.010±0.033	0.000	45.787±0.041	0.000	45.74±0.22	−44.52±0.25	90.26±0.33
340.00		42.513±0.025	0.001	46.913±0.035	0.000	42.50±0.21	−45.08±0.27	87.58±0.35
360.00		41.252±0.020	0.001	48.045±0.034	0.001	39.65±0.20	−45.58±0.30	85.24±0.36
380.00		40.190±0.020	0.003	49.185±0.034	0.002	37.13±0.20	−46.03±0.32	83.16±0.38
400.00		39.299±0.020	0.005	50.332±0.036	0.004	34.90±0.20	−46.42±0.34	81.32±0.40
420.00		38.550±0.022	0.010	51.482±0.038	0.008	32.90±0.20	−46.77±0.37	79.66±0.42
440.00		37.920±0.024	0.016	52.632±0.041	0.013	31.10±0.21	−47.07±0.39	78.17±0.44
460.00		37.396±0.028	0.026	53.780±0.044	0.020	29.48±0.22	−47.35±0.41	76.83±0.47
480.00		36.959±0.035	0.039	54.925±0.050	0.030	28.02±0.23	−47.59±0.44	75.61±0.49
500.00		36.598±0.044	0.056	56.066±0.058	0.042	26.69±0.24	−47.80±0.46	74.49±0.51
520.00		36.302±0.060	0.077	57.201±0.071	0.056	25.48±0.25	−47.99±0.48	73.46±0.54
540.00		36.063±0.080	0.102	58.328±0.089	0.074	24.37±0.26	−48.15±0.51	72.52±0.56
560.00		35.865±0.104	0.133	59.439±0.111	0.093	23.35±0.28	−48.31±0.54	71.65±0.59
580.00		35.703±0.130	0.169	60.535±0.138	0.116	22.40±0.30	−48.45±0.56	70.85±0.62
600.00	c	35.571±0.162	0.208	61.614±0.169	0.139	21.52±0.32	−48.58±0.59	70.10±0.64
620.00	c	35.462±0.195	0.253	62.674±0.204	0.166	20.70±0.35	−48.70±0.62	69.41±0.67
640.00	c	35.374±0.235	0.305	63.715±0.242	0.195	19.93±0.38	−48.82±0.66	68.75±0.70
660.00	c	35.295±0.276	0.359	64.730±0.284	0.223	19.20±0.42	−48.94±0.69	68.15±0.72
680.00	c	35.225±0.323	0.419	65.720±0.332	0.252	18.51±0.46	−49.07±0.73	67.58±0.75
700.00	c	35.167±0.376	0.491	66.692±0.386	0.290	17.85±0.50	−49.19±0.78	67.04±0.78

TABLE 1.15. Continued

$\frac{T}{K}$		$\frac{\Delta_0^T H_m^\circ}{RT}$	$\frac{\Delta_{imp} H_m^\circ}{RT}$ [a]	$\frac{\Delta_0^T S_m^\circ}{R}$	$\frac{\Delta_{imp} S_m^\circ}{R}$ [b]	$\frac{\Delta_f H_m^\circ}{RT}$	$\frac{\Delta_f S_m^\circ}{R}$	$\frac{\Delta_f G_m^\circ}{RT}$
				Indoline				
298.15	[c]	39.610±0.065	0.000	42.064±0.069	0.000	48.72±0.23	−45.64±0.21	94.36±0.30
300.00	[c]	39.467±0.062	0.000	42.166±0.067	0.000	48.36±0.22	−45.70±0.21	94.06±0.30
320.00	[c]	38.079±0.035	0.001	43.277±0.043	0.001	44.79±0.21	−46.27±0.23	91.06±0.30
340.00	[c]	36.904±0.022	0.002	44.378±0.034	0.002	41.65±0.20	−46.78±0.24	88.43±0.31
360.00	[c]	35.918±0.019	0.005	45.470±0.033	0.004	38.88±0.19	−47.25±0.26	86.14±0.33
380.00		35.086±0.019	0.009	46.557±0.034	0.007	36.42±0.19	−47.68±0.28	84.10±0.34
400.00		34.389±0.022	0.016	47.642±0.036	0.013	34.23±0.19	−48.06±0.31	82.29±0.36
420.00		33.802±0.027	0.026	48.719±0.040	0.020	32.26±0.19	−48.41±0.33	80.67±0.38
440.00		33.315±0.033	0.039	49.792±0.046	0.030	30.48±0.19	−48.72±0.35	79.21±0.40
460.00	[d]	32.908±0.044	0.057	50.859±0.055	0.042	28.88±0.20	−49.01±0.37	77.89±0.42
480.00	[d]	32.574±0.058	0.079	51.919±0.067	0.057	27.43±0.21	−49.26±0.39	76.69±0.44
500.00	[d]	32.301±0.075	0.106	52.971±0.083	0.075	26.10±0.22	−49.49±0.41	75.59±0.46

[a] Gas-imperfection correction to the ideal-gas enthalpy.

[b] Gas-imperfection correction to the ideal-gas entropy.

[c] Values at this temperature were calculated with extrapolated vapor pressures calculated from the fitted Cox coefficients.

[d] Values at this temperature were calculated with graphically extrapolated values of the liquid-phase heat capacities.

2.1. APPROACH

The general approach to the calculation of thermodynamic equilibria in organic systems has been outlined in previous reports from this research group.[1,2]§ The methodology can be summarized as follows. For the general reaction:

$$\text{reactant} + n\ H_2 \Leftrightarrow \text{product(s)}$$

a pseudo-equilibrium constant, K', is defined such that

$$\ln K' = -\Delta_r G^\circ_m/RT + n\ [\ln(P_{H_2}/P^\circ)] \qquad (2.1)$$

where P° is the standard state pressure used in the thermodynamic calculations (101.325 kPa, or 1 atmosphere in this report). As has been noted in previous reports,[1,2] if ln K' is plotted versus 1/T, near linear curves are obtained. This facilitates extrapolation of the experimental values obtained at relatively low temperature into the range of commercial processes.

Figure 2.1 shows the reaction scheme considered here for the hydrodenitrogenation (HDN) of indole. In this part of the report equilibrium constants are calculated for each reaction depicted. These calculations require the Gibbs energy of formation, $\Delta_f G^\circ_m$, as a function of temperature for each compound. Details of the methods used to derive the $\Delta_f G^\circ_m$ values (listed in table 2.1¶) are given in this section. The equilibrium constants derived here are used and discussed in PART 3 of this report.

2.2 GIBBS ENERGIES OF FORMATION

INDOLE

The thermodynamic properties for 2-methylindole reported in Part 1 were used to derive estimates of the Gibbs energies of formation of the parent molecule; indole. The intrinsic molar entropy increments for methyl substitution in the ideal-gas state for substituted benzenes, naphthalenes, and phenanthrenes were reported in reference 3. Those results were determined from:

$$\Delta S^\circ_m(-CH_2-) = S^\circ_m\{A(CH_3)_n\} - S^\circ_m(AH_n) + R\ \ln(\sigma_2/\sigma_1) \qquad (2.2)$$

where AH_n represents an unsubstituted compound with n hydrogens to be replaced by methyl groups and σ_1 and σ_2 are the ratios of the symmetry number to the number of

---

§ References are listed in numerical order at the end of this Part.

¶ Tables appear at the end of this Part.

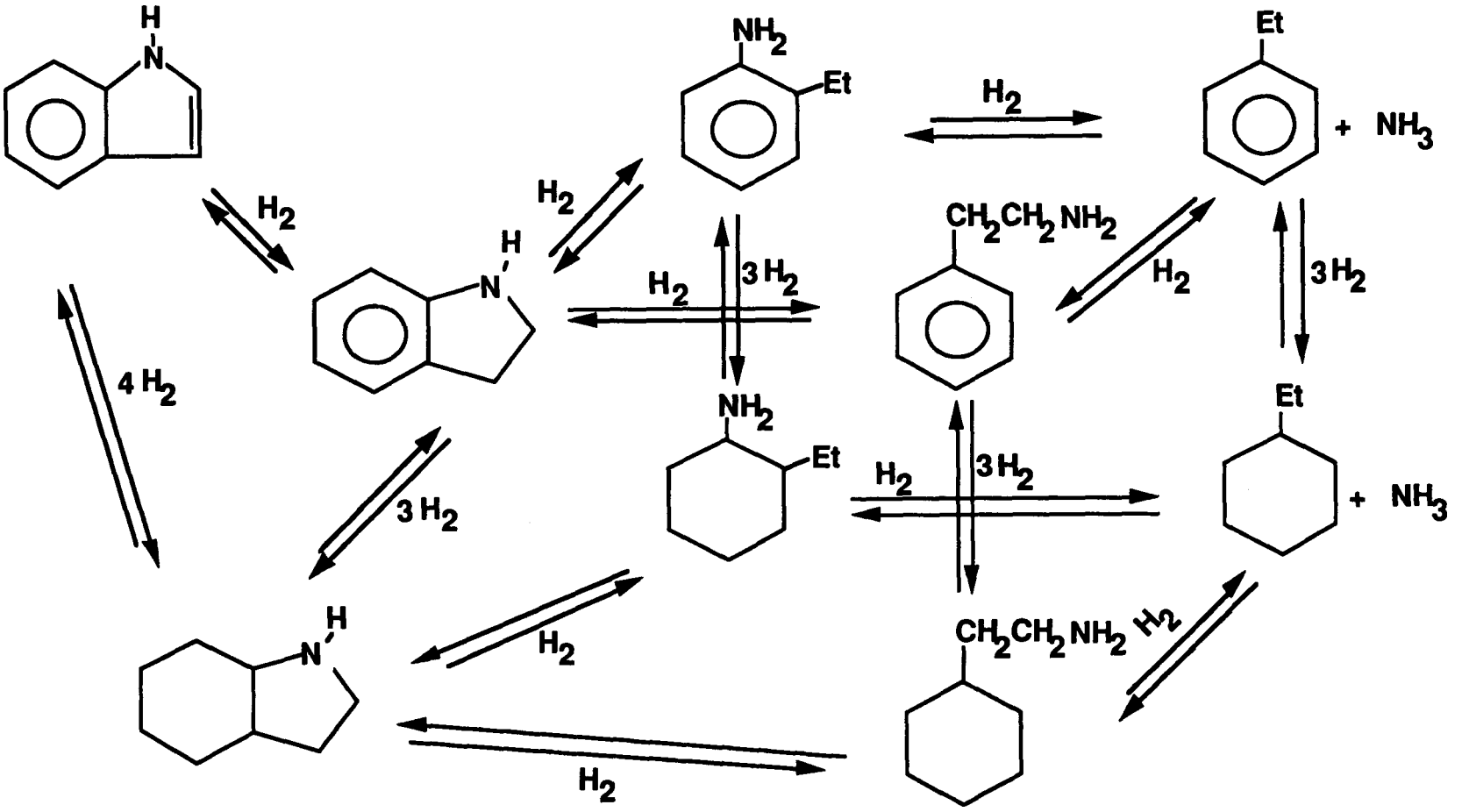

FIGURE 2.1. Hydrodenitrogenation (HDN) reaction scheme for indole

optical isomers for the unsubstituted and methyl substituted compounds, respectively. In the absence of steric hindrance, values of 5.5 R, 6.4 R, and 7.2 R were obtained for ΔS°_{m} $(-CH_2-)$ at 300 K, 400 K, and 500 K, respectively. Analogous calculations using 2,5-dimethylpyrrole, 2,4-dimethylpyrrole, and 3-methylpyrrole[4] gave values of 5.65 R, 6.48 R, 7.27 R at 300 K, 400 K, and 500 K, respectively with, in addition, values of 7.96 R at 600 K, and 8.36 R at 700 K. Applying equation **2.2** to 2-methylindole in conjunction with σ values of three for 2-methylindole and one for indole gave the ideal-gas entropies reported in table 2.2. Ideal-gas entropies of formation for indole were calculated using the estimated entropies and the corresponding entropies for equilibrium hydrogen, graphite, and nitrogen reported in the JANAF tables.[5] The results are reported in column 5 of table 2.2.

The condensed-phase standard enthalpy of formation of indole was determined by Good[6] but, in the absence of either a reliable enthalpy of sublimation, or accurate vapor pressure measurements, reliable calculation of the corresponding ideal-gas enthalpy of formation is suspect. Estimation of the ideal-gas enthalpy of formation of indole at 298.15 K from that of 2-methylindole (given in table 1.15 PART 1) was made by comparison of the enthalpies of formation of 2,5-dimethylpyrrole,[6] 2,4-dimethylpyrrole,[4] 3-methylpyrrole,[4] and pyrrole.[7] A value $\Delta_f H^{\circ}_{m}$ $(C_8H_7N,g, 298.15\ K)$ = (162.0±1.25) $kJ \cdot mol^{-1}$ was estimated. Ideal-gas enthalpies of formation for indole at temperatures other than 298.15 K were calculated using enthalpy of formation increments obtained in the same manner as the entropy increments detailed above. The results are reported in column 6 of table 2.2.

INDOLINE

The ideal-gas Gibbs energies of formation for indoline reported in table 1.15 are reproduced in table 2.1.

PERHYDROINDOLE

The ideal-gas thermodynamic functions for perhydroindole were estimated using the group additivity parameters derived by Benson.[8] The parameters used are listed in tables 2.3 and 2.4. The estimation methodology has been detailed in reference 9. Perhydroindole has two optical isomers; so $R \cdot \ln 0.5$ was subtracted from the intrinsic entropies derived by summation of the groups to obtain the ideal-gas entropies.

2-ETHYLANILINE

Draeger[10] lists ideal-gas thermodynamic functions for 2-methylaniline derived from spectroscopic measurements and an estimated enthalpy of formation at 298.15 K.

Calculation of the thermodynamic functions for 2-methylaniline were repeated using an experimentally determined ideal-gas enthalpy of formation; $\Delta_f H^\circ_m$ (C_7H_9N, g, 298.15 K) = 52.58±0.92 kJ·mol,$^{-1}$ (unpublished enthalpy of combustion measurements and vapor-pressure measurements in the temperature range 290 to 500 K). The method of increments[11] was then used to estimate the thermodynamic functions for 2-ethylaniline applying the formula:

2-ethylaniline = 2-methylaniline + ethylbenzene – toluene **(2.3)**

This notation is the same as that used in reference 11. Values for the entropies and enthalpies of formation for ethylbenzene and toluene were taken from Stull, Westrum, and Sinke.[11]

2-PHENYLETHYLAMINE

The method of increments was used to estimate the ideal-gas thermodynamic functions for 2-phenylethylamine using the formula:

2-phenylethylamine = ethylamine + ethylbenzene – ethane – {R ln2} . **(2.4)**

In **2.4** the symmetry numbers from left to right are 2, 3, 6, and 18, respectively. The logarithmic term corrects for the discrepancy in total symmetry numbers for over-all and internal rotation in the formula **2.4** as written. It is necessary in the calculations of the entropies but not the enthalpies of formation. Values from Stull, Westrum, and Sinke[11] were used for ethylamine, ethylbenzene and ethane.

ETHYLBENZENE, ETHYLCYCLOHEXANE AND AMMONIA

The values given in table 2.1 are those given by Stull, Westrum, and Sinke.[11]

2-CYCLOHEXYLETHYLAMINE

The method of increments was used to estimate the ideal-gas thermodynamic functions for 2-cyclohexylethylamine applying the formula:

2-cyclohexylethylamine = ethylamine + ethylcyclohexane – ethane + {R ln2} . **(2.5)**

In **2.5** the symmetry numbers from left to right are 1, 3, 3, and 18, respectively. Values from Stull, Westrum, and Sinke[11] were used for ethylamine, ethylcyclohexane and ethane.

CIS- AND TRANS-2-ETHYLCYCLOHEXYLAMINE

The method of increments was used to estimate the ideal-gas thermodynamic functions for both the cis- and trans isomers of 2-ethylcyclohexylamine using the formula:

$$\text{cis or trans 2-ethylcyclohexylamine} = \text{cis or trans-2-methylethylcyclohexane} + \text{2-aminopropane} - \text{2-methylpropane} - \{R \ln 3\} . \qquad (2.6)$$

In **2.6** the symmetry numbers from left to right are 3, 9, 9, and 81, respectively. The thermodynamic functions for cis or trans-2-methylethylcyclohexane were derived using the formula:

$$\text{cis or trans 2-methylethylcyclohexane} = \text{cis or trans-1,2-dimethylcyclohexane} + \text{ethylcyclohexane} - \text{methylcyclohexane} . \qquad (2.7)$$

In **2.7** the symmetry numbers from left to right are 9, 9, 3, and 3, respectively. All values used in applying formulas **2.6** and **2.7** were taken from Stull, Westrum, and Sinke[11] except for 2-aminopropane where the values of Scott[12] were used.

TRANS-2-ETHYL-1-METHYLCYCLOPENTANE

The method of increments was used to estimate the ideal-gas thermodynamic functions for trans 2-ethylmethylcyclopentane using the formula:

$$\text{trans-2-ethyl-1-methylcyclopentane} = \text{trans-1,2-dimethylcyclopentane} + \text{ethylcyclopentane} - \text{methylcyclopentane} - \{R \ln 2\} . \qquad (2.8)$$

In **2.8** the symmetry numbers from left to right are 9, 18, 3, and 3, respectively. All values used in calculations applying formula **2.8** were taken from Stull, Westrum, and Sinke.[11]

UNCERTAINTIES IN ESTIMATED VALUES

The uncertainty interval (one standard deviation) in the estimated Gibbs energies of formation reported in table 2.1 varies, depending on the degree of estimation used in the derivations. Since the values were used to determine Gibbs energies of reaction in a closed system (in the thermodynamic sense). the uncertainties in the enthalpies and entropies of the elements as assessed by JANAF[5] cancel in the equilibrium calculations reported in Part 3. Neglecting the uncertainties in the elements the uncertainty interval for the dimensionless Gibbs energies of formation (i.e., $\Delta_f G^\circ_m/RT$) for indoline reported in table 2.1 is ±0.2 over the temperature range reported. A constant value of ±0.2 for the uncertainty interval in the dimensionless Gibbs energies of formation was

assumed for ethylbenzene, ethylcyclohexane, and ammonia, all of which were taken from the values reported by Stull, Westrum, and Sinke.[11]

For indole the uncertainty interval is a combination of the uncertainty interval for 2-methylindole (ranging from 0.25 at 290 K, 0.20 at 400 K, to 0.50 at 700 K), the uncertainty in the free rotation methyl increments, and the uncertainty in the estimation of the ideal-gas enthalpy of formation at 298.15 K. On the basis of several similar estimations for organic nitrogen-containing compounds, the largest uncertainty is in the estimation of the ideal-gas enthalpy of formation, ±1.25 kJ·mol.$^{-1}$ On that basis the uncertainty in the dimensionless Gibbs energies of formation of indole is ±0.5.

The uncertainty interval in the ideal-gas enthalpy of formation for 2-methylaniline (obtained from the combustion calorimetry and vapor-pressure measurements) was ±0.20. Uncertainties on the derived entropy and enthalpy increments were an order of magnitude less than that value. Therefore, the assigned uncertainty was ±0.2

For perhydroindole, group-contribution parameters were applied to calculate the thermodynamic functions. In a recent topical report[9] on the biphenyl/hydrogen system, an uncertainty interval of ±R in entropies estimated using group-additivity parameters was assessed. Hence, the uncertainty interval assigned to the dimensionless Gibbs energies of formation for perhydroindole was ±1.4.

For the remaining compounds listed in table 2.1 the method of increments was used to estimate the Gibbs energies of formation. Uncertainty intervals in the dimensionless Gibbs energies of formation obtained applying this method are generally of the order of ±1.0, and that value has been assigned in subsequent calculations in this report.

2.3 GIBBS ENERGIES OF REACTION

Values of $\Delta_r G^\circ_m$ for each of the reactions depicted in figure 2.1 are listed in table 2.5. Equations in the form of **2.1** are listed in table 2.6 for each of the reactions (the reaction numbers given in table 2.6 are those used to denote the equilibria in table 2.5). Part 3 of the report discusses chemical equilibria in the indole/hydrogen network calculated using the Gibbs energies of reaction.

2.4 DISCUSSION

The American Petroleum Institute (API) Monograph Series Publication 719[13] lists thermodynamic properties for indole obtained from the literature and estimated. The ideal-gas thermodynamic functions reported in the monograph were derived "using molecular property data from reference 14" (molecular structure of the crystal) "and estimated by analogy with carbazole." Details of the estimation method are not provided. The enthalpy of formation at 298.15 K for indole in the ideal-gas state derived here, $\Delta_f H^\circ_m$ (C_8H_7N,g 298.15 K) = (162.0±1.25) kJ·mol,$^{-1}$ is 6.5 kJ·mol^{-1} more positive than that given in the API monograph.[13] Such a difference in enthalpies of formation shifts the indole/indoline equilibrium by a relatively large amount. Using the results developed here (equation 1, table 2.6), under 60 atmospheres hydrogen pressure, the calculated temperature at which an equimolar mixture of indole and indoline exists is 530 K. If the API enthalpy of formation is used in conjunction with the entropies derived here (see below), the calculated temperature for equimolar amounts of indole and indoline becomes 443 K, a shift of approximately 90 K.

Figure 2.2 compares the entropies obtained here with those given in the monograph. The difference in entropy {S°_m(this research) – S°_m(API)} ranges from 0.59R at 300 K to 1.31R at 700 K. In a recent paper from this laboratory, Collier[15] reported a complete frequency assignment for indole with the important low wave-number frequencies all given for the gas phase (hence, removing errors due to the well-known liquid-to-gas phase frequency shifts which occur for the lowest frequencies). Values for the ideal-gas entropy for indole obtained using his frequencies and the same molecular structure as that used in the API monograph[13,14] are also plotted in figure 2.2. The agreement between the spectroscopic entropies and those determined in this research is good (all differences are less than twice the standard deviation assigned to the estimated indole values). Differences between the spectroscopic values and those reported in the API monograph, in contrast, are large, ranging from 0.49R at 300 K to 0.66R at 700 K. Table 2.7 shows the change in the calculated temperature for an equimolar mixture of indole and indoline under 60 atmospheres hydrogen pressure compared to that derived using equation 1 from table 2.6 for various combinations of estimated entropies and enthalpies of formations. Note the 130 K range in the calculated temperature which arises from the various combinations.

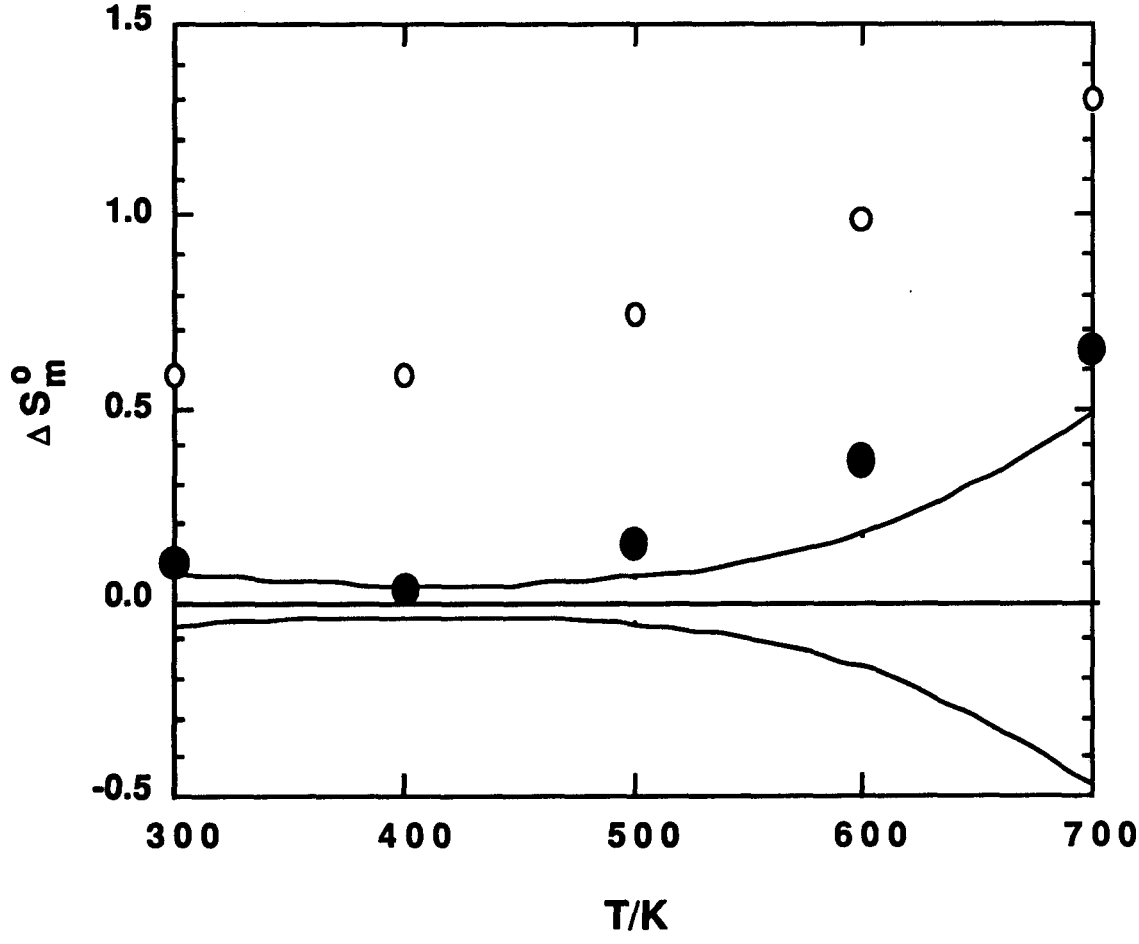

Figure 2.2 Comparison of estimated and spectroscopic ideal-gas entropies for indole. The solid lines represent the error limits (one standard deviation) assigned to the entropies estimated in this report. The open circles are values of $\{S^\circ_m$(this research) – S°_m(reference 13)$\}/R$. The filled circles are of $\{S^\circ_m$(this research) – S°_m(spectroscopic, reference 15)$\}/R$.

2.5 REFERENCES

1. Steele, W. V.; Archer, D. G.; Chirico, R. D.; Strube, M. M. *Comparison of the Thermodynamics of Nitrogen and Sulfur Removal in Heavy Oil Upgrading. Part 1. Acyclic and Monocyclic Compounds.* NIPER-264. July **1987.**
2. Chirico, R. D.; Hossenlopp, I. A.; Nguyen, A.; Strube, M. M.; Steele, W. V. *Thermodynamic Studies Related to the Hydrogenation of Phenanthrene.* NIPER-247. Published by DOE Fossil Energy, Bartlesville Project Office. Available from NTIS Report No. DE-8687001252, April **1987.**
3. Chirico, R. D.; Hossenlopp, I. A.; Nguyen, A.; Steele, W. V.; Gammon, B. E. *J. Chem. Thermodynamics* **1989**, 21, 179.
4. Steele, W. V.; Chirico, R. D.; Collier, W. B.; Hossenlopp, I. A.; Nguyen, A.; Strube, M. M. *Thermochemical and Thermophysical Properties of Organic Nitrogen Compounds Found in Fossil Materials.* NIPER-188. Published by DOE Fossil Energy, Bartlesville Project Office. Available from NTIS Report No. DE-8687001204, November **1986.**
5. Chase, M. W., Jr. ; Davies, C. A.; Downey, J. R., Jr.; Frurip, D. J.; McDonald, R. A.; Syverud, A. N. *JANAF Thermochemical Tables.* Third edition. *J. Phys. Chem. Ref. Data* **1985**, 14, supplement No. 1, 2 volumes..
6. Good, W. D. *J. Chem. Eng. Data* **1972**, 17, 28.
7. Scott, D. W.; Berg, W. T.; Hossenlopp, I. A.; Hubbard, W. N.; Messerly, J. F.; Todd, S. S.; Douslin, D. R.; McCullough, J. P.; Waddington, G. *J. Phys. Chem.* **1967**, 71, 2263.
8. Benson, S. W. *Thermochemical Kinetics.* 2nd edition. Wiley: New York, **1976.**
9. Chirico, R. D.; Steele, W. V. "*Thermodynamic Equilibria in the Biphenyl/ Hydrogen System. The Power and Limitations of Group Additivity Estimations,*" Topical Report NIPER-403, March **1989.**
10. Draeger, J. A. *J. Chem. Thermodynamics* **1984**, 16, 1067.
11 Stull, D. R.; Westrum, E. F., Jr.; Sinke, G. C. *The Chemical Thermodynamics of Organic Compounds.* Wiley. New York. **1969.**
12. Scott, D. W. *J. Chem. Thermodynamics* **1971**, 3, 843.
13. Kudchadker, S. A.; Wilhoit, R. C. *Indole* API Monograph Series Publication 719. American Petroleum Institute, Washington, D.C. April **1982.**
14. Lautie, A.; Lautie, M. F.; Gruger, A.; Fakhri, S. A. *Spectrochim. Acta* **1980**, 36A, 85.
15. Collier, W. B. *J. Chem. Phys.* **1988**, 88, 7295.

TABLE 2.1 Gibbs energies of formation for intermediates and products in the HDN of indole [a,b] (R = 8.31441 $J \cdot K^{-1} \cdot mol^{-1}$ and p° = 101.325 kPa)

T/K	$\Delta_f G^\circ_m$ /RT				
	Indole	Indoline	Perhydroindole	2-Ethylaniline	2-Phenylethylamine
300	97.07	94.06	63.36	69.14	81.60
400	81.28	82.29	68.89	66.30	75.14
500	72.00	75.59	72.68	65.00	71.72
600	65.75		74.93	64.20	69.69
700	61.25		77.83	63.81	68.37
800			80.51	63.61	67.42
900			82.85	63.49	66.75
1000			85.32	63.43	66.24
	Ethylbenzene	2-CHEA	trans-2-ECHA	cis-2-ECHA	Ethylcyclohexane
300	52.69	45.28	40.24	42.95	16.38
400	50.07	59.27	56.30	58.22	34.20
500	48.92	68.38	66.73	68.22	45.58
600	48.41	74.82	74.01	75.22	53.53
700	48.15	79.58	79.28	80.29	59.36
800	48.04	83.21	83.39	84.26	63.82
900	48.00	86.07	86.62	87.38	67.33
1000	48.01	88.37	89.18	89.85	70.15
	trans 2-EMCP	NH_3			
300	19.61	-6.41			
400	36.12	-1.72			
500	46.43	1.21			
600	53.69	3.22			
700	59.05	4.71			
800	63.04	5.84			
900	66.44	6.74			
1000	69.09	7.47			

[a] The derivation of the values is described in the text.

[b] 2-CHEA 2-cyclohexylethylamine
2-ECHA 2-ethylcyclohexylamine
2-EMCP 2-ethyl-1-methylcyclopentane

TABLE 2.2 Estimation of the ideal-gas thermodynamic functions for indole [a,b]
($R = 8.31441\ J{\cdot}K^{-1}{\cdot}mol^{-1}$ and $p^\circ = 101.325$ kPa)

T/K	$\{\Delta S_m^\circ(-CH_2-)\}/R$	$\Delta_0^T S_m^\circ/R$ 2-methylindole	$\Delta_0^T S_m^\circ/R$ indole	$\Delta_f S_m^\circ/R$ indole	$\Delta_f H_m^\circ/RT$ indole
300	5.65	44.67	40.12	−32.07	65.00
400	6.48	50.33	44.95	−34.08	47.20
500	7.27	56.07	49.90	−35.10	36.90
600	7.96	61.61	54.75	−35.59	30.16
700	8.36	66.69	59.43	−35.73	25.52

[a] Values for 2-methylindole from table 1.15.

[b] See text for details of the estimation methods used.

TABLE 2.3. Group-additivity terms for estimation of ideal-gas thermodynamic properties of perhydroindole at 298.15 K. [a] ($R = 8.31441\ J \cdot K^{-1} \cdot mol^{-1}$ and $p^\circ = 101.325\ kPa$)

Group	$\frac{\Delta_0^T S_m^\circ}{R}$	$\frac{\Delta_f H_m^\circ}{RT}$
$(C)\text{-}(C)_2(H)_2$	4.74	−8.32
$(C)\text{-}(C)_3(H)$	−6.07	−3.21
$(C)\text{-}(C)_2(N)(H)$	−5.89	−8.78
$(C)\text{-}(C)(N)(H)_2$	4.93	−11.14
$(N)\text{-}(C)_2(H)$	7.75	15.09
Cyclohexane ring correction	9.46	0.0
Pyrrolidine ring correction	13.44	11.48

[a] Values from reference 8.

TABLE 2.4. Coefficients in polynomial representation of group-additivity terms from reference 8 for estimation of ideal-gas heat capacities. [a]
($R = 8.31441\ J \cdot K^{-1} \cdot mol^{-1}$)

Group	A	10^2B	10^6C
$(C)-(C)_2(H)_2$	0.40	1.92	−7.29
$(C)-(C)_3(H)$	−0.54	2.00	−9.42
$(C)-(C)_2(N)(H)$	−0.87	2.23	−11.24
$(C)-(C)(N)(H)_2$	−0.37	2.17	−8.99
$(N)-(C)_2(H)$	2.84	1.03	−2.68
Cyclohexane ring correction	−12.07	2.34	−9.00
Pyrrolidine ring correction	−9.14	1.07	−3.64

[a] $C_P/R = A + BT + CT^2$

TABLE 2.5 Gibbs energies of reactions in the HDN of indole [a]
(R = 8.31441 $J \cdot K^{-1} \cdot mol^{-1}$ and p° = 101.325 kPa)

T/K	$-\Delta_r G^\circ_m$ /RT				
Reaction # / T/K	1	2	3	4	5
300	3.01	33.71	30.70	24.92	12.46
400	−1.01	12.39	13.40	15.99	7.15
500	−3.59	−0.68	2.91	10.59	3.87

Reaction # / T/K	6	6A	7	8	9
300	23.12	20.41	18.08	28.90	22.86
400	12.59	10.67	9.62	10.00	17.95
500	5.95	4.46	4.30	−1.73	14.87
600	0.92	−0.29	0.11	−9.81	12.57
700	−1.45	−2.46	−1.75	−15.47	10.95
800	−2.88	−3.75	−2.70	−19.78	9.73

Reaction # / T/K	10	10A	11 and 14	12 and 13	15
300	30.27	32.98	36.32	35.32	−3.23
400	23.82	25.74	15.87	26.79	−1.92
500	19.94	21.43	3.34	21.59	−0.85
600	17.26	18.47	−5.13	18.06	−0.16
700	15.21	16.22	−11.21	15.51	0.31
800	13.73	14.60	−15.79	13.54	0.78

[a] See table 2.6 for reaction corresponding to each number.

TABLE 2.6 Equations to represent the equilibria given in figure 2.1

Reaction #	
1	INDOLE → INDOLINE
	$\ln K' = (4940\pm300)/T - (13.42\pm0.81) + [\ln(P_{H_2} / P^\circ)]$
2	INDOLE → PERHYDROINDOLE
	$\ln K' = (25770\pm840)/T - (52.15\pm2.24) + \{4\ [\ln(P_{H_2} / P^\circ)]\}$
3	INDOLINE → PERHYDROINDOLE
	$\ln K' = (20830\pm790)/T - (38.73\pm2.11) + \{3\ [\ln(P_{H_2} / P^\circ)]\}$
4	INDOLINE → 2-ETHYLANILINE
	$\ln K' = (10740\pm160)/T - (10.89\pm0.42) + [\ln(P_{H_2} / P^\circ)]$
5	INDOLINE → 2-PHENYLETHYLAMINE
	$\ln K' = (6435\pm570)/T - (8.98\pm1.53) + [\ln(P_{H_2} / P^\circ)]$
6	PERHYDROINDOLE → trans-2-ETHYLCYCLOHEXYLAMINE
	$\ln K' = (12030\pm485)/T - (17.66\pm0.94) + [\ln(P_{H_2} / P^\circ)]$
6A	PERHYDROINDOLE → cis-2-ETHYLCYCLOHEXYLAMINE
	$\ln K' = (11161\pm490)/T - (17.44\pm1.00) + [\ln(P_{H_2} / P^\circ)]$
7	PERHYDROINDOLE → 2-CYCLOHEXYLETHYLAMINE
	$\ln K' = (10280\pm490)/T - (16.26\pm1.00) + [\ln(P_{H_2} / P^\circ)]$
8	2-ETHYLANILINE → trans-2-ETHYLCYCLOHEXYLAMINE
	$\ln K' = (23500\pm340)/T - (49.08\pm0.65) + \{3\ [\ln(P_{H_2} / P^\circ)]\}$

TABLE 2.6 Continued

Reaction #	
9	2-ETHYLANILINE → ETHYLBENZENE + AMMONIA
	$\ln K' = (6415\pm250)/T + (1.74\pm0.48) + [\ln(P_{H_2} / P^\circ)]$
10	trans-2-ETHYLCYCLOHEXYLAMINE → ETHYLCYCLOHEXANE + AMMONIA
	$\ln K' = (8010\pm250)/T + (3.73\pm0.47) + [\ln(P_{H_2} / P^\circ)]$
10A	cis-2-ETHYLCYCLOHEXYLAMINE → ETHYLCYCLOHEXANE + AMMONIA
	$\ln K' = (8930\pm250)/T + (3.39\pm0.48) + [\ln(P_{H_2} / P^\circ)]$
11	2-PHENYLETHYLAMINE → 2-CYCLOHEXYLETHYLAMINE
	$\ln K' = (25100\pm330)/T - (47.09\pm0.64) + \{ 3 [\ln(P_{H_2} / P^\circ)]\}$
12	2-PHENYLETHYLAMINE → ETHYLBENZENE + AMMONIA
	$\ln K' = (10520\pm245)/T + (0.40\pm0.47) + [\ln(P_{H_2} / P^\circ)]$
13	2-CYCLOHEXYLETHYLAMINE → ETHYLCYCLOHEXANE + AMMONIA
	$\ln K' = (10520\pm245)/T + (0.40\pm0.47) + [\ln(P_{H_2} / P^\circ)]$
14	ETHYLBENZENE → ETHYLCYCLOHEXANE
	$\ln K' = (25100\pm330)/T - (47.09\pm0.64) + \{ 3 [\ln(P_{H_2} / P^\circ)]\}$
15	ETHYLCYCLOHEXANE → trans-2-ETHYL-1-METHYLCYCLOPENTANE
	$\ln K' = (3.02\pm0.14) - (1900\pm720)/T$

TABLE 2.7 Effect of changes in the enthalpies and entropies of formation of indole on calculated equilibria in the indole/indoline system [a,b]

$\Delta_f S^\circ_m/R$	$\Delta_f H^\circ_m/RT$	T/K
NIPER	NIPER	530
NIPER	API	443
API	NIPER	575
API	API	475

[a] NIPER = values determined in this report.

[b] API = values given in reference 13.

[c] T = calculated temperature at which equimolar amounts of indole and indoline are present at thermodynamic equilibrium under 60 atmospheres hydrogen pressure.

3.1. THERMODYNAMIC EQUILIBRIA

This section discusses the various thermodynamic equilibria in the reaction scheme depicted in figure 2.1. Calculations were done using the equations listed in table 2.6 of Part 2. In the calculations only the more stable *trans-* isomer of 2-ethyl-cyclohexylamine was considered.

INDOLE/INDOLINE EQUILIBRIA

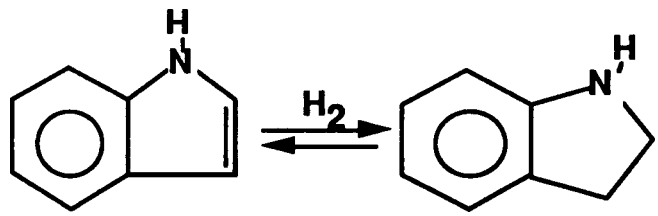

The initial step in the reaction scheme given in figure 2.1 (indole → indoline) is a reversible reaction in the temperature range of interest, favored by **low** temperature. Figure 3.1 shows the percentage of indoline at thermodynamic equilibrium for the hydrogenation of indole in the temperature interval 400 to 800 K for hydrogen pressures of 20, 60, and 100 atmospheres. The equilibrium percentages of indoline were calculated using the equation for reaction 1 given in table 2.6 of Part 2 of this report:

$$\ln K' = (4940\pm300)/T - (13.42\pm0.81) + [\ln(P_{H_2}/P^\circ)]. \qquad 3.1$$

At 473 K (200° C) 20 atmospheres of hydrogen is needed to obtain a 50/50 mole per cent mixture of indole and indoline. At higher temperatures greater hydrogen pressures are required to maintain the equimolar mixture at equilibrium: at 530 K (257° C) 60 atm. H_2 is required: at 560 K (287° C) 100 atm. H_2 is required.

For the calculation of equilibrium concentrations, thermodynamic information of the highest quality is required. This is demonstrated in the lower graph in figure 3.1, which shows the effect of the assigned uncertainties given to the constants in the equation **3.1**. At 530 K and 60 atm. H_2 the calculated equilibrium mixture contains 50 mole per cent of each component. However, the estimated uncertainty intervals on the equation parameters cause the upper and lower bounds of that result to be 80 and 20 per cent indoline, respectively, at equilibrium. (The majority of the uncertainty arises in the estimation of the methyl increment to the ideal-gas enthalpy of formation for 2-methylindole, which was used to derive the indole value.) If the ideal-gas

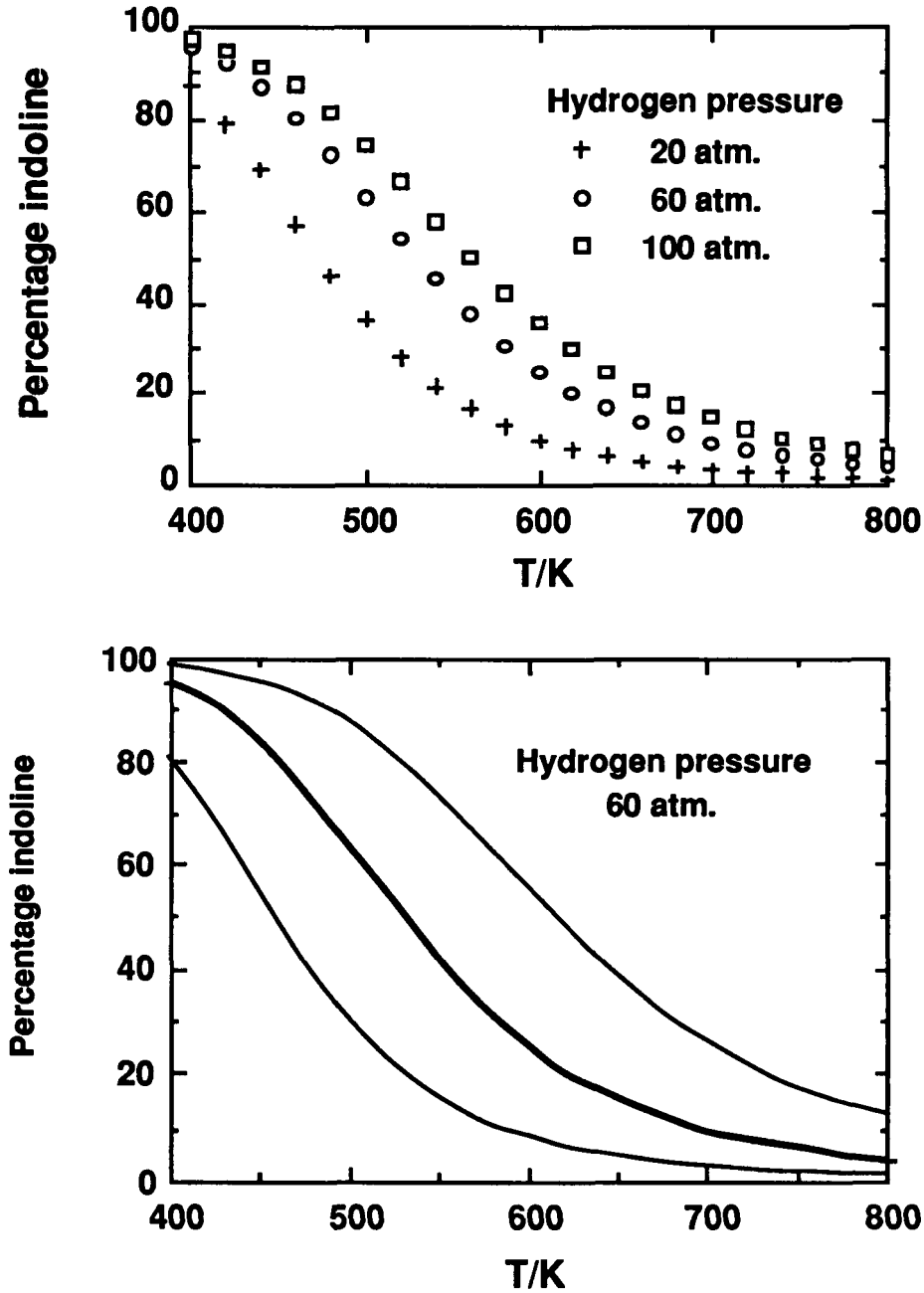

FIGURE 3.1 Thermodynamic equilibrium concentrations of indoline calculated using equation **3.1**. The upper graph shows the variation of the equilibrium concentration of indoline with both hydrogen pressure and temperature. In the lower graph the thick solid line represents equation **3.1**. The thin solid lines represent the upper and lower bounds of that equation derived using the assigned uncertainty intervals.

thermodynamic properties for indole were measured directly and not estimated as per Part 2, then the uncertainty interval would be much smaller, of the order of ±10 per cent. · Alternatively, the effect of the uncertainty interval can be thought of as an uncertainty in the temperature associated with a particular product ratio. For example, with the uncertainty estimates for equation **3.1**, the temperature associated with a 50/50 mixture is known only within a 150 K range. Directly measured values would reduce this to less than a 50 K range.

COMPARISON WITH LITERATURE EQUILIBRIUM MEASUREMENTS

Two batch-reactor experimental studies[1,2]§ of the indole/indoline equilibrium were found in the literature. Odebunmi and Ollis[1] studied the HDN of indole over a sulfided $CoMo/Al_2O_3$ catalyst, and they reported indole/indoline equilibrium molar ratios at 523, 548, 573, and 623 K and 69 atm. H_2 pressure. These are plotted (filled circles) in figure 3.2.

Shaw and Stapp[2] measured equilibria in the indole/indoline/hydrogen system in the temperature range 416 to 573 K, with hydrogen pressures of 83 to 179 atmospheres. Their results are plotted (open circles) in figure 3.2. The solid line in figure 3.2 represents equation **3.1**. Except for two outlying points (in both cases perhydroindole was observed in the reaction products) agreement between the results of Shaw and Stapp,[2] Odebunmi and Ollis,[1] and the thermodynamic equilibrium calculations is excellent.

In figure 3.2 the dashed lines represent the upper and lower bounds of the thermodynamic equilibrium calculations using the assigned uncertainty intervals given in equation **3.1**. From the experimental equilibrium measurements it would seem that the assigned uncertainties are unduly pessimistic. If the uncertainty intervals in equation **3.1** were reduced by a factor of 5 the calculated equilibria would still be in excellent accord with the experimentally determined values. There are insufficient corroborative thermodynamic data available to justify reducing the uncertainty intervals at this time.

---

§ References are listed in numerical order at the end of this Part.

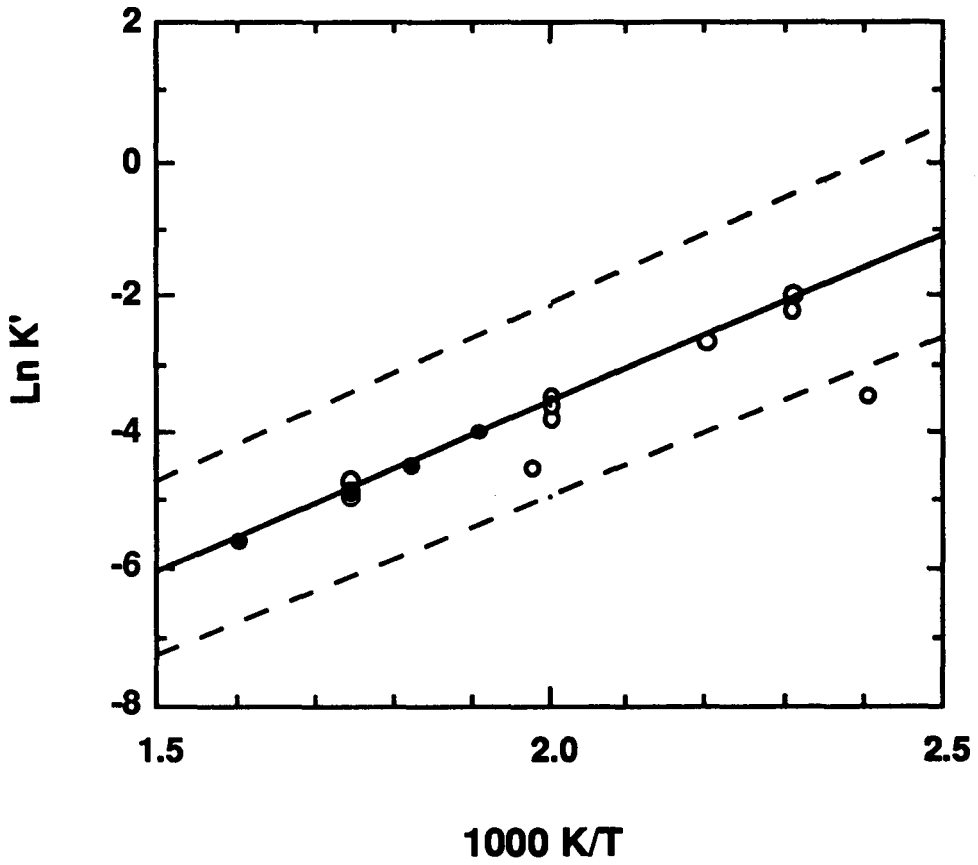

FIGURE 3.2 The indole/indoline equilibrium. Comparison of the indole/indoline experimental equilibrium results of Odebunmi and Ollis (reference 1: filled circles) and Shaw and Stapp (reference 2: open circles) with values derived from the thermodynamic results given in Part 2 of this report. The solid line represents equation 3.1. The dashed lines represent the upper and lower bounds of that equation derived using the assigned uncertainty intervals.

Upon formation of indoline the HDN of indole can proceed along two pathways; one immediate ring opening leaving the aromatic ring intact, and the second through ring saturation to form perhydroindole and subsequently cyclohexane derivatives. Equilibria for these paths are considered separately and comparisons are made with reaction studies to elucidate the most likely path.

INDOLE/INDOLINE/PERHYDROINDOLE/2-ETHYLCYCLOHEXYLAMINE/2-CYCLOHEXYL-ETHYLAMINE EQUILIBRIA

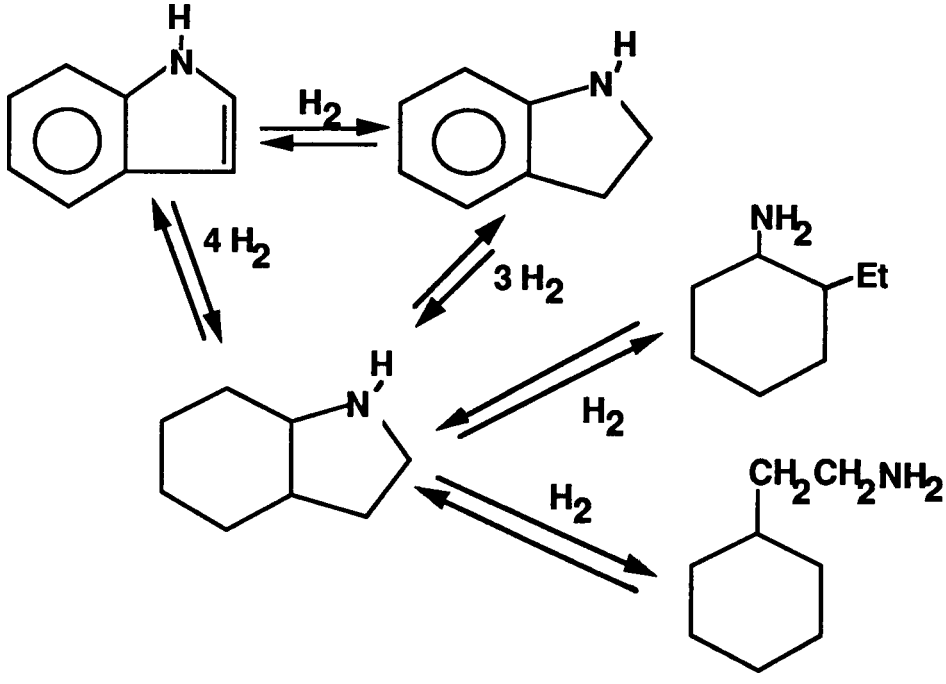

In this system, at thermodynamic equilibrium, the major product at low temperatures (less than 600 K) is 2-ethylcyclohexylamine. The results of the equilibria calculations are shown in figure 3.3. Above 600 K, under 20 atm. H_2, the concentration of indole (open triangles in figure 3.3) rises rapidly reaching approximately 100 per cent at 800 K (top graph). At 800 K, as the hydrogen pressure is increased the concentration of indole drops, falling to 80 mole per cent at 60 atm. H_2 (center graph), and to approximately 30 mole per cent at 100 atm. H_2 (bottom graph). Note, under thermodynamic equilibrium conditions, the concentration of 2-cyclohexylethylamine (squares in figure 3.3), while lower than that of 2-ethylcyclohexylamine (filled circles), is still significant, peaking in the range 20 to 30 mole per cent as the hydrogen pressure increases from 20 to 100 atm. H_2. At equilibrium, concentrations of indoline and perhydroindole remain very low across the ranges of hydrogen pressure and temperatures studied. The maximum concentrations of

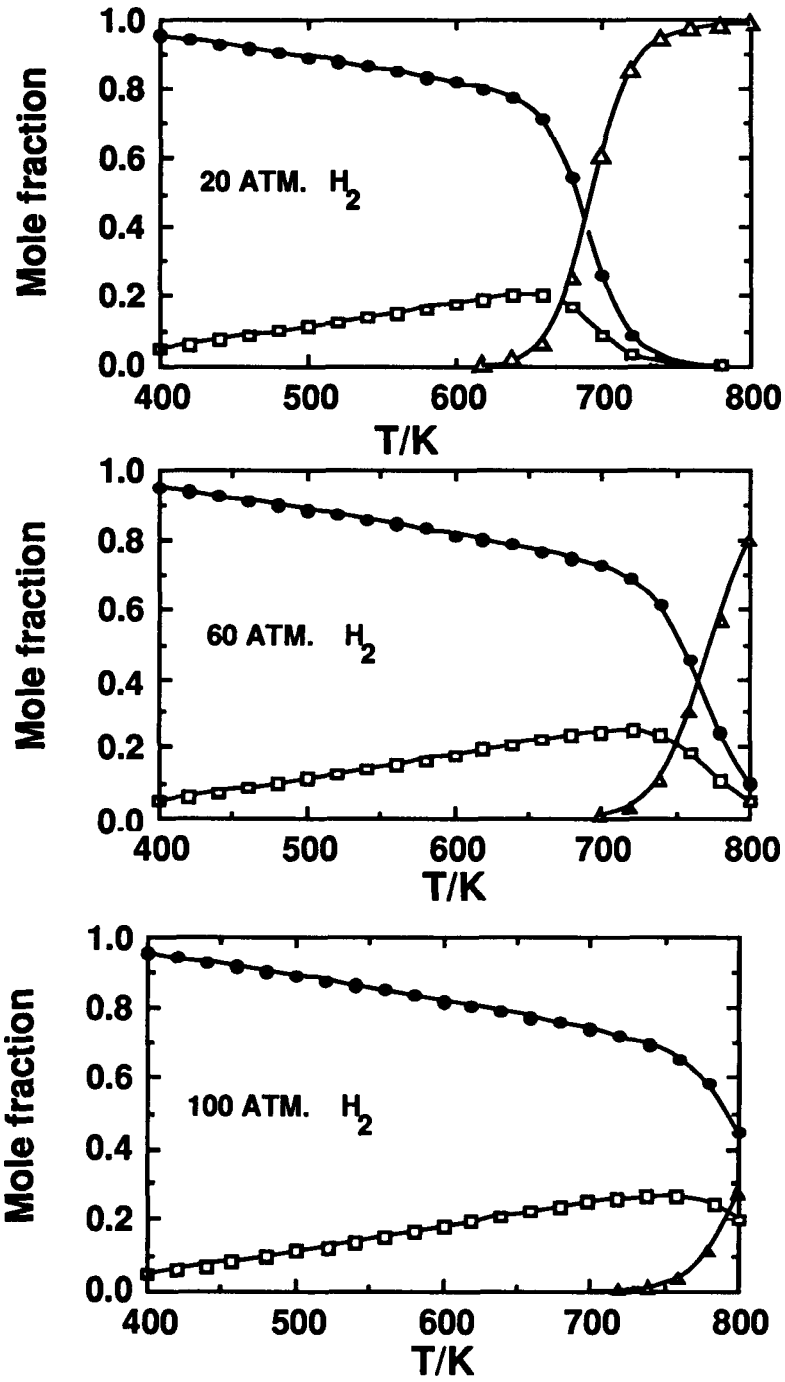

FIGURE 3.3 Calculated thermodynamic equilibrium concentrations in the indole/indoline/perhydroindole/2-ethylcyclohexylamine/2-cyclohexylethylamine system. The squares represent 2-cyclohexylethylamine; the filled circles 2-ethylcyclohexylamine; the triangles indole. Concentrations of indoline and perhydroindole were too small to represent on these plots (see text).

indoline and perhydroindole calculated were 3 per cent (at 60 atm. H_2) and 6 per cent (at 100 atm. H_2), respectively.

EQUILIBRIA INVOLVING PERHYDROINDOLE

Perhydroindole has never been detected in the HDN of indole.[1,3-9] This is consistent with the calculations reported here, where perhydroindole is a minor product in the equilibria studied; the reaction proceeds through perhydroindole to either 2-ethylcyclohexylamine or 2-cyclohexylethylamine to ethylcyclohexane. The fact that all the research studies of the HDN reaction also showed the presence of 2-ethylaniline precludes the perhydroindole pathway being the **sole** reaction pathway.

The failure to find any perhydroindole in the reaction products does *not* preclude it from being **one** of the pathways to the products. However, if it was a major pathway, the presence of 2-cyclohexylethylamine in the reaction products would be highly probable. Only Hartung et al.[3] have observed 2-cyclohexylethylamine in the reaction products from the HDN of indole. Hartung et al[3] described the hydrogenolysis of indole dissolved in a middle distillate fuel (they called the solvent "furnace oil") under 205 atmospheres hydrogen pressure at 588 K. The initial concentration of nitrogen in the reaction mixture was 5000 ppm, and the reaction was quenched when the nitrogen level reached 4300 ppm. Therefore, the presence of a range of reaction intermediates was expected and subsequently confirmed. The major products in the study by Hartung et al.[3] were indoline and 2-ethylaniline with no perhydroindole detected.

INTERPLAY OF THERMODYNAMICS AND KINETICS IN THE HDN REACTION SCHEME

Thermodynamic equilibria calculations can be used as an aid in the interpretation of kinetics and catalyst intercomparison studies. The analysis of the reaction scheme below serves as an example of how thermodynamics and kinetics work "hand in hand."

INDOLE/INDOLINE/2-ETHYLANILINE/2-PHENYLETHYLAMINE EQUILIBRIA

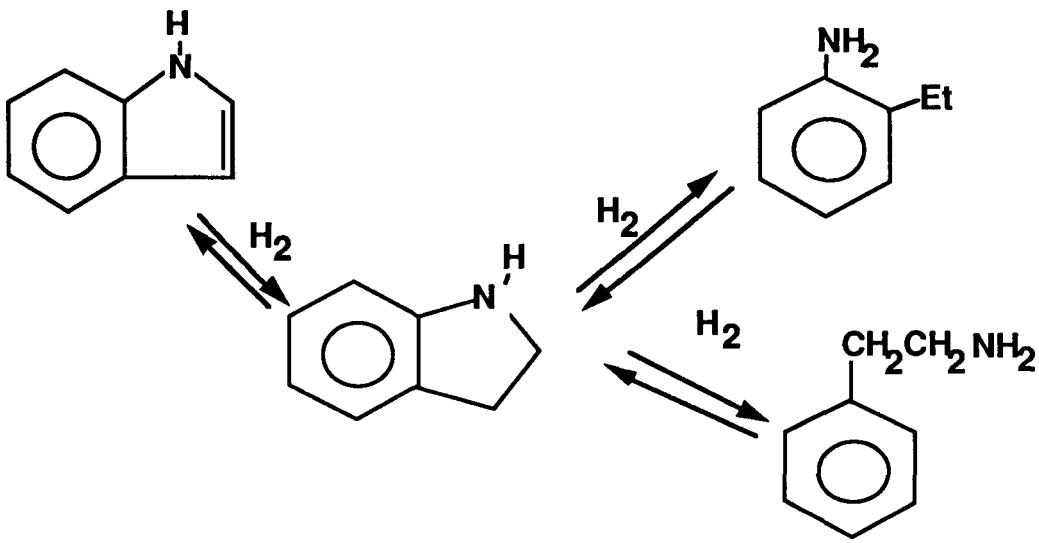

Thermodynamic equilibria calculations on this system (20 to 100 atm. H_2; 400 to 800 K) revealed only two components present in concentrations greater than 3 mole per cent, 2-ethylaniline and indole. Figure 3.4 summarizes the results of the equilibria calculations under 20 atm. H_2. At 20 atm. H_2 at 800 K the equilibrium mixture contained 76 mole per cent 2-ethylaniline, three mole per cent 2-phenylethylamine, and 21 mole per cent indole. At 100 atm. H_2 pressure the mole per cent values were 96, 3, and 1 respectively.

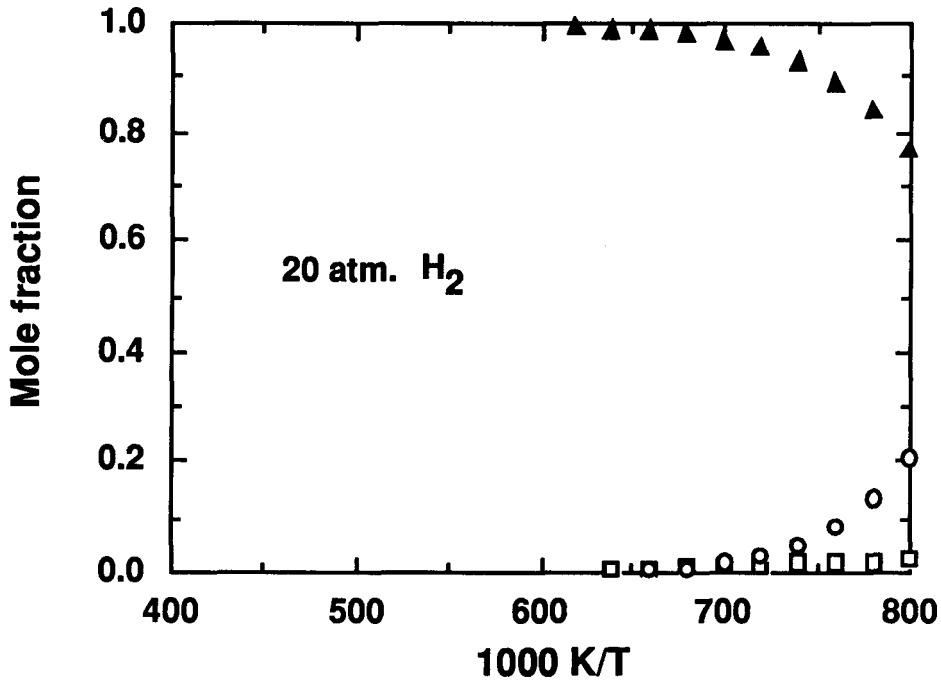

FIGURE 3.4 Calculated thermodynamic equilibrium concentrations in the indole/indoline/2-ethylaniline/2-phenylethylamine system. The filled triangles represent 2-ethylaniline; the squares 2-phenylethylamine; and the circles indole.

The majority of the HDN reaction schemes for indole published in the literature show the presence of a thermodynamic equilibrium between indole and indoline during the reaction.[1, 4-8] The effect of the indole/indoline reversible reaction step on the HDN of indole depends on the kinetics of the various steps.¶ If the initial heterocyclic ring hydrogenation is rate determining (k_2 is large relative to k_1 in footnote ¶), then the indoline would react as it is formed, and the position of the equilibrium would have *no* effect on the overall HDN reaction. In mathematical terms:

$$-\frac{d[\text{indole}]}{dt} = \frac{k_1 k_2 [\text{indole}][H_2]^2 - k_{-1} k_{-2} [\text{2-ethylaniline}]}{k_{-1} + k_2 [H_2]} ,$$

simplifies to $k_1[\text{indole}][H_2]$. If, however, the hydrogenolysis (ring-opening to form either 2-ethylaniline or 2-phenylethylamine) reaction is rate limiting (i.e., k_1 is large relative to k_2), then the reversible reaction can reach equilibrium, and the overall kinetics of HDN will show a thermodynamic dependence. Further, if the hydrogenolysis reaction is rate determining, then as the temperature is raised the thermodynamic equilibrium will move towards the formation of indole offsetting the

---

¶ In the kinetics of:

$$\text{indole} \underset{k_{-1}}{\overset{k_1}{\rightleftharpoons}} \text{indoline} \underset{k_{-2}}{\overset{k_2}{\rightleftharpoons}} \text{2-ethylaniline} ,$$

the rate of reaction of indole is given by:

$$-\frac{d[\text{indole}]}{dt} = k_1[\text{indole}][H_2] - k_{-1}[\text{indoline}] ,$$

and the rate of reaction of indoline is given by:

$$-\frac{d[\text{indoline}]}{dt} = k_{-1}[\text{indoline}] + k_2[\text{indoline}][H_2] - k_1[\text{indole}][H_2] - k_{-2}[\text{2-ethylaniline}] .$$

Under steady state conditions for indoline $\frac{d[\text{indoline}]}{dt} = 0$ and hence

$$[\text{indoline}] = \frac{k_1[\text{indole}][H_2] - k_{-2}[\text{2-ethylaniline}]}{k_{-1} + k_2[H_2]} ,$$

and on substitution for the indoline concentration

$$-\frac{d[\text{indole}]}{dt} = \frac{k_1 k_2 [\text{indole}][H_2]^2 - k_{-1} k_{-2} [\text{2-ethylaniline}]}{k_{-1} + k_2 [H_2]} .$$

The thermodynamic equilibrium constant K_{th}, is defined as the ratio of the rates of the forward and reverse reactions. Hence, for the indole/indoline equilibrium

$$K_{th} = \frac{k_1[\text{indole}][H_2]}{k_{-1}[\text{indoline}]} .$$

normal increase in the kinetic rate constant.§ Then, the reaction rate will go through a *maximum* as the temperature is increased, all other reaction conditions remaining constant.

Skala et al.[7] made studies on the HDN of indole, quinoline, and lauronitrile ($CoMo/Al_2O_3$, $NiMo/Al_2O_3$ sulfided catalysts, 473 to 643 K, 79 atm. H_2). Their results for indole HDN are given in figures 9, 11, and 13 of reference 7. The figures show a maximum concentration of indoline at 523 K in agreement with the comments above with respect to the interplay of increasing rate constant with temperature but decreasing equilibrium concentration of indoline. Such a maximum was also observed in the HDN of quinoline by Satterfield and coworkers.[10]

The indoline hydrogenolysis reaction "masks" the indole/indoline hydrogenation equilibrium, and hence, the equilibrium constants determined from analyses of batch reaction products (pseudo-equilibrium constants, K_{ps}) are somewhat lower than the thermodynamic equilibrium constants (K_{th}). The extent to which the "pseudo equilibrium constants" are lower than the thermodynamic values is a measure of the degree of "masking." If the rate of the hydrogenolysis (ring-opening) reaction was very slow relative to the hydrogenation(i.e., k_2 in footnote ¶ very small relative to k_1), then K_{ps} would equal K_{th}. If the hydrogenolysis reaction was relatively very fast (k_2 very large relative to k_1) then, there would be 100 percent "masking," and the indoline would react as it was formed producing no thermodynamic restrictions on the overall rate of HDN.

Olive et al.[6] in a study of the HDN of both indole and 2-ethylaniline on sulfided $CoMo/Al_2O_3$, $NiMo/Al_2O_3$, and NiW/Al_2O_3 catalysts at temperatures of 573 and 613 K, (34 and 69 atmospheres H_2 pressure) reported pseudo first-order rate constants¥ for both the forward and reverse reactions in the hydrogenation step for indole. These are reproduced in table 3.1. Also reported in table 3.1 column 6 are the corresponding "pseudo equilibrium constants"(K_{ps}) for the indole/indoline reaction. The ratio of K_{ps} to K_{th} for each set of reaction conditions is given in column 8 of table 3.1. The ratios K_{ps}/K_{th} reported in table 3.1 show that for the $NiMo/Al_2O_3$ catalyst, increasing the hydrogen pressure fails to significantly promote the hydrogenolysis reaction relative to the hydrogenation equilibrium (0.54 cf. 0.56 in the ratio K_{ps}/K_{th}; the first two items

---

§ The Arrhenius rate expression, $k = A \exp(-E_a/RT)$, denotes the relationship between temperature and the rate of a chemical reaction. A good "rule of thumb" is that the rate doubles for every 10 to 20 Kelvin rise in temperature.

¥ The rate of reaction is second order, rate=k[indoline][H_2], but the concentration of hydrogen is so large that rate=k'[indoline] where k'=k[H_2]. k' is the pseudo first-order rate constant.

in table 3.1); increasing the temperature does promote hydrogenolysis (0.56 cf. 0.41 in the ratio K_{ps}/K_{th}; the second and third entries in table 3.1). The fourth entry shows that the $CoMo/Al_2O_3$ catalyst promoted hydrogenolysis (ring opening) slightly more than the $NiMo/Al_2O_3$ catalyst (0.49 cf. 0.56 in the K_{ps}/K_{th} ratio). The final entry shows that for the NiW/Al_2O_3 catalyst the rate of the hydrogenolysis reaction was slow compared to the hydrogenation reaction rate and hence K_{ps}/K_{th} was larger (0.63).

TABLE 3.1. Indole/indoline concentration ratios at equilibrium and pseudo equilibrium. [a,b]

Catalyst	T / K	P_{H_2} atm.	$k_1[P_{H_2}]$ $\cdot 10^3$	$k_{-1}+k_2[P_{H_2}]$ $\cdot 10^3$	K_{ps}	K_{th}	K_{ps}/K_{th}
$NiMo/Al_2O_3$	573	34	3	20	0.15	0.28	0.54
$NiMo/Al_2O_3$	573	69	7	22	0.32	0.57	0.56
$NiMo/Al_2O_3$	613	69	13	101	0.13	0.32	0.41
$CoMo/Al_2O_3$	573	69	4.5	16	0.28	0.57	0.49
NiW/Al_2O_3	573	69	8	22	0.36	0.57	0.63

[a] Rate data from reference 6.

[b] K_{ps} (the pseudo-equilibrium constant calculated from rate data) = $k_1[P_{H_2}]/(k_{-1}+k_2[P_{H_2}])$.

[c] K_{th} equals thermodynamic equilibrium constant calculated from equation **3.1**.

The above discussion highlights the interplay between thermodynamics and kinetics in catalyst evaluation. Thermodynamics gives values of equilibrium product ratios (K_{th} values in this case) which are independent of catalytic effects. A kinetic analysis of a particular series of experiments, performed under varying conditions and in the presence of different catalysts, gives values of pseudo equilibrium product ratios (K_{ps} values in the above example). Of great interest in the development of a catalyst is the ratio of the two values K_{ps} and K_{th} which in this case is a measure of the relative abilities of hydrogenation and hydrogenolysis. The NiW/Al_2O_3 catalyst was the "best" hydrogenation catalyst, while the $CoMo/Al_2O_3$ catalyst proved to be the "best" hydrogenolysis catalyst.

The thermodynamic calculations show a predominance of 2-ethylaniline over 2-phenylethylamine in the reaction scheme, when the calculations are curtailed at that step (see figure 3.4). In agreement with that result, the HDN studies reported in the literature fail to note 2-phenylethylamine as a product or reaction intermediate.

NITROGEN REMOVAL STEP IN THE HDN OF INDOLE

The steps in the reaction scheme where ammonia is formed will now be considered. In analogy to the indole/indoline/2-ethylaniline system there is an interplay between the thermodynamics of the various reactions and the relative kinetics of each step.

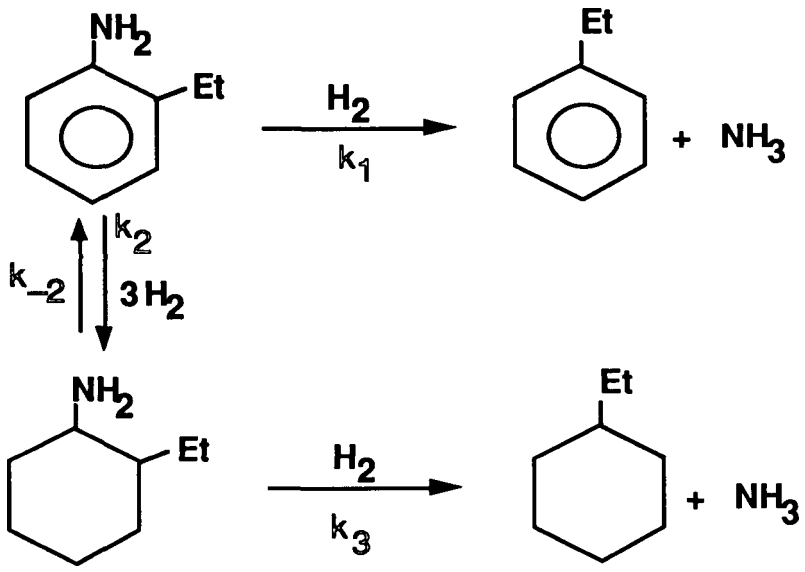

Figure 3.5 shows the results of equilibria calculations for the above system. The thermodynamic equilibria calculations can be summarized as follows. **The reaction steps which form ammonia are thermodynamically irreversible.** Ethylcyclohexane is favored by low temperatures and high H_2 pressure. Ethylbenzene is favored by high temperatures and low H_2 pressures. Stern,[5] while discussing reaction networks in catalytic hydrodenitrogenation in the presence of several different sulfided catalysts ($CoMo/Al_2O_3$, $NiMo/Al_2O_3$, Re/Al_2O_3, $CoRe/Al_2O_3$, 623 K, 68 atm. H_2), reported that reaction of 2-ethylcyclohexylamine occurred very rapidly ("under the conditions employed 95 per cent is converted by the time the reaction conditions are attained"). This is in agreement with the formation of ethylcyclohexane being thermodynamically irreversible.

In the literature there appear at first sight to be contradictions in what are the major products in the HDN of indole. Studies reported by Rollman[4], Stern,[5] Olive et al.[6] and Skala et al.[7] all list ethylcyclohexane as the major HDN product. In contrast to those studies Odebunmi and Ollis,[1] Aboul-Gheit and Aboul,[8] and Shaw[9] reported 2-ethylaniline as a major product of the HDN reaction. Thermodynamics shows that both reaction pathways are possible in the pressure and temperature regimes used in the

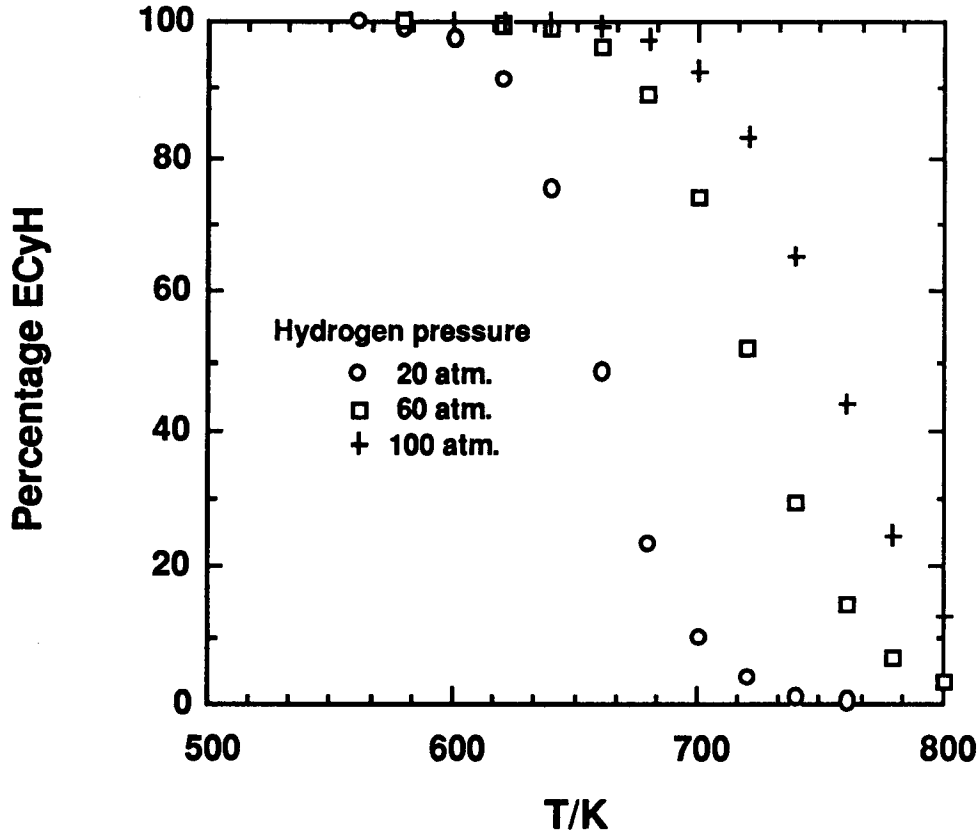

FIGURE 3.5 Calculated thermodynamic equilibrium concentrations of ethylcyclohexane (ECyH).

experimental studies. Which pathway is taken depends on the relative rates of the reactions.¶¶ The kinetic expression of the rate of removal of 2-ethylaniline is

$$-\frac{d[2\text{-EA}]}{dt} = k_1[2\text{-EA}][H_2] + k_2[2\text{-EA}][H_2]^3 .$$

In the absence of a catalyst, the rate constants k_1 and k_2 will be directly related to the relative bond energies. For aliphatic amines the bond dissociation energy D_{298}, is in the range 300 to 350 kJ·mol.$^{-1}$ However, for aniline the C-NH_2 bond dissociation energy is 427 kJ·mol.$^{-1}$ Therefore, the activation energy E_a, for the pathway to ethylbenzene is significantly higher than that to ethylcyclohexane. For the reaction to give ethylbenzene as the major product the catalyst needs to lower the E_a for that pathway more than it lowers E_a for the ethylcyclohexane pathway. The Re/C catalyst used by Shaw,[9] in a study of the HDN of 1,2,3,4-tetrahydroquinoline, quinoline, indole, and 2-ethylaniline is an example of such a catalyst. For each compound studied, aromatic hydrocarbon selectivity was high; 68 to 77 mole per cent. However, when the catalyst was presulfided, 2-ethylaniline was converted mainly to ethylcyclohexane (76 moles per cent), the opposite of that observed when no sulfur was present. In an earlier report[11] on the HDN and HDS of acyclic and monocyclic compounds the present authors speculated that Re/Mo catalyst would also be effective in promoting the ethylbenzene pathway.

¶¶ In the kinetics the rate of reaction of 2-ethylaniline (2-EA) is given by

$$-\frac{d[2\text{-EA}]}{dt} = k_1[2\text{-EA}][H_2] + k_2[2\text{-EA}][H_2]^3 - k_{-2}[2\text{-ethylcyclohexylamine}]$$

and the rate of reaction of 2-ethylcyclohexylamine (2-ECyHA) is given by

$$-\frac{d[2\text{-ECyHA}]}{dt} = k_{-2}[2\text{-ECyHA}] + k_3[2\text{-ECyHA}][H_2] - k_2[2\text{-EA}][H_2]^3$$

Under steady state conditions for 2-ECyHA $\frac{d[2\text{-ECyHA}]}{dt} = 0$ and hence

$$[2\text{-ECyHA}] = \frac{k_2[EA][H_2]^3}{k_{-2} + k_3[H_2]} .$$

On substitution for the 2-ECyHA concentration, with k_3 being large relative to the other rate constants (Stern[5]),

$$-\frac{d[2\text{-EA}]}{dt} = k_1[2\text{-EA}][H_2] + k_2[2\text{-EA}][H_2]^3$$

is obtained.

ALKYL-SUBSTITUTED CYCLOPENTANE FORMATION

Catalysts used in HDN reactions contain acidic sites (Al_2O_3) and hence, promote the isomerization of cyclohexanes to cyclopentanes. In PART 2 the Gibbs energies of reaction for the isomerization of ethylcyclohexane to trans-2-ethyl-1-methylcyclopentane are listed in table 2.6. The results show that the isomerization reaction is favored at temperatures greater than 630 K. Note that the reaction is independent of hydrogen pressure.) None of the HDN studies reported in the literature list alkyl substituted cyclopentanes among the reaction products. However, alkyl substituted cyclopentanes occur among the reaction products in studies on the HDN of quinoline[10] and it is probable that their presence was overlooked in the analysis of the reaction products.

THERMODYNAMIC EQUILIBRIA REACTION SCHEME

The thermodynamic equilibria reaction scheme shown in figure 2.1 can be simplified considerably in light of the above calculations. A revised thermodynamic equilibria reaction scheme for the HDN of indole is shown in figure 3.6.

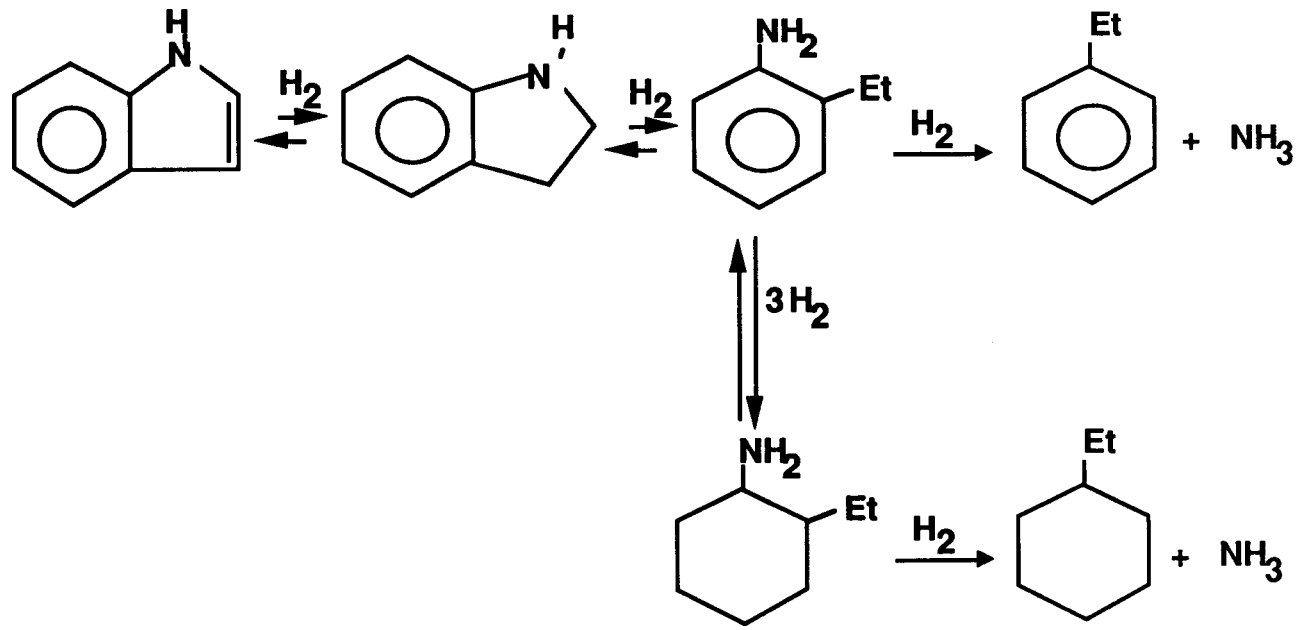

FIGURE 3.6 Revised thermodynamic equilibrium scheme for the HDN of indole.

3.2 REFERENCES

1. Odebunmi, E. O.; Ollis, D. F. *J. Catalysis* **1983**, 80, 76.
2. Shaw, J. E.; Stapp, P. R. *J. Heterocyclic Chem.* **1987**, 24, 1477.
3. Hartung, G. K.; Jewell, D. M.; Larson, O. A.; Flinn, R. A. *J. Chem. Eng. Data* **1961**, 6, 477.
4. Rollman, L. D. *J. Catalysis* **1977**, 46, 243.
5. Stern, E. W. *J. Catalysis* **1979**, 57, 390.
6. Olive, J.-L.; Biyoko, S.; Moulinas, C.; Geneste, P. *Applied Catalysis* **1985**, 19, 165.
7. Skala, D. U.; Saban, M. D.; Jovanovia, J. A.; Meyn, V. W.; Rahimian, I. G.-H. *Ind. Eng. Chem. Res.* **1988**, 27, 1186.
8. Aboul-Gheit, A. K.; Aboul, I. K. *J. Inst. Petroleum* **1973**, 59, 188.
9. Shaw, J. E. *Fuel* **1988**, 67, 1706.
10. Satterfield, C. N.; Yang, S. H. *Ind. Eng. Chem. Process Des. Dev.* **1984**, 23, 11
11. Steele, W. V.; Archer, D. G.; Chirico, R. D.; Strube, M. M. *Comparison of Thermodynamics of Nitrogen and Sulfur Removal in Heavy Oil Upgrading. Part 1. Acyclic and Monocyclic Compounds.* NIPER-264, July **1987**.

SUMMARY and HIGHLIGHTS

NEW THERMODYNAMIC PROPERTY MEASUREMENTS FOR KEY COMPOUNDS

- Ideal-gas thermodynamic properties for indoline and 2-methylindole were determined based on accurate calorimetric measurements. The calorimetric measurements are the first reported in the literature on indole derivatives.
- Values for the critical properties of 2-methylindole are listed. Again, these are the first reported experimental measurements for an organic molecule containing a pyrrole ring other than the parent molecule pyrrole and a few alkyl-substituted derivatives.
- The experimentally determined critical properties for 2-methylindole act as "cornerstones" in the estimation of the critical properties of other substituted indoles. (Critical properties are often used by engineers in corresponding-states correlations for the estimation of a variety of physical properties.)
- The experimental measurements on 2-methylindole were used to estimate the ideal-gas thermodynamic properties for indole. (The derived values are in serious disagreement with estimated values reported previously in the literature.) In contrast, the agreement between the estimated thermodynamic properties for indole obtained in this research and those calculated via statistical thermodynamics is good (see below).

THERMODYNAMIC PROPERTY ESTIMATES FOR MOLECULES INVOLVED IN THE HDN OF INDOLE

- A reaction network for the HDN of indole was chosen, and Gibbs energies of formation for each of the molecules in the reaction scheme were estimated using group-additivity methodology.
- Gibbs energies of reaction were calculated for each of the steps in a reaction scheme for the HDN of indole.

THERMODYNAMIC EQUILIBRIA CALCULATIONS AND THEIR RELATIONSHIP TO KINETICS AND CATALYST STUDIES

- Thermodynamic equilibria calculations on the indole/indoline/hydrogen system are in excellent accord with literature batch-reaction studies. This is strong evidence in favor of the accuracy of the indole properties estimated in this report.
- Thermodynamic equilibria calculations showed perhydroindole to be a possible intermediate in the HDN of indole. The failure of researchers to find perhydroindole in the reaction products in kinetic studies does *not* preclude it from being **one** of the pathways to the products. The fact that all published

studies of the HDN reaction showed the presence of 2-ethylaniline precludes the perhydroindole pathway from being the **sole** reaction pathway.

- The interplay between thermodynamic equilibria and the rate of reaction of each of the elementary steps in a reaction scheme was shown using the indole/indoline/2-ethylaniline/2-phenylethylamine system as an example. Using results reported in the literature, thermodynamics and kinetics were combined to elucidate the relative effectiveness of a series of catalysts to effect hydrogenation and hydrogenolysis reactions. For the example given a NiW/Al_2O_3 catalyst was the "best" hydrogenation catalyst, while a $CoMo/Al_2O_3$ catalyst proved to be the "best" hydrogenolysis catalyst.
- The thermodynamic equilibria calculations showed that the reaction steps which form ammonia are thermodynamically irreversible. Such reactions are under kinetic control. The products of the HDN of 2-ethylaniline depend on the catalyst used to effect the reaction. A catalyst that will reduce the activation energy for the pathway to ethylbenzene more than the pathway to ethylcyclohexane will be the "best" for aromatic production (i.e., hydrogen saving). A report in the literature shows a Re/C catalyst can be used to give high yield of aromatics in HDN reactions. It is speculated that a Re/Mo catalyst would be more effective in the presence of sulfur-containing compounds.

☆U.S. GOVERNMENT PRINTING OFFICE: 1989-661-023/00027